Chapter 11
Particle Beam Parameters

Particle beams are characterized by a set of quantifying parameters being either constants of motion or functions varying from point to point along a beam transport line. The parameters may be a single particle property like the betatron function which is the same for all particles within a beam or quantities that are defined only for a collection of particles like beam sizes or beam intensity. We will define and derive expressions for such beam parameters and use them to characterize particle beams and develop methods for manipulation of such parameters.

11.1 Definition of Beam Parameters

Particle beams and individual particles are characterized by a number of parameters which we use in beam dynamics. We will define such parameters first before we discuss the determination of their numerical value.

11.1.1 Beam Energy

Often we refer to the energy of a particle beam although we actually describe only the nominal energy of a single particle within this beam. Similarly, we speak of the beam momentum, beam kinetic energy or the velocity of the beam, when we mean to say that the beam is composed of particles with nominal values of these quantities. We found in earlier chapters that the most convenient quantity to characterize the "energy" of a particle is the momentum for transverse beam dynamics and the kinetic energy for acceleration. To unify the nomenclature it has become common to use the term energy for both quantities noting that the quantity of pure momentum should be multiplied with the velocity of light (cp) to become

H. Wiedemann, *Particle Accelerator Physics*, Graduate Text in Physics,
https://doi.org/10.1007/978-3-319-18317-6_11

dimensionally correct. Thus, the particle momentum is expressed in the dimension of an energy without being numerically identical either to the total energy or the kinetic energy but approaching both for highly relativistic energies.

11.1.2 Time Structure

A true collective beam parameter is the time structure of the particle stream. We make the distinction between a continuous beam being a continuous flow of particles and a bunched beam. Whenever particles are accelerated by means of rf-fields a bunched beam is generated, while continuous beams can in general be sustained only by dc accelerating fields or when no acceleration is required as may be true for a proton beam in a storage ring. A pulsed beam consists of a finite number of bunches or a continuous stream of particles for a finite length of time. For example, a beam pulse from a linear accelerator is made up of a finite string of micro bunches generated by rf-accelerating fields.

11.1.3 Beam Current

The beam intensity or beam current is expressed in terms of an electrical current using the common definition of the ratio of the electrical charge passing by a current monitor per unit time. For bunched beams the time span during which the charge is measured can be either shorter than the duration of the bunch or the beam pulse or may be long compared to both. Depending on which time scale we use, we define the bunch current or peak current, the pulse current or the average current respectively.

In Fig. 11.1 the general time structure of bunched beams is shown. The smallest unit is the microbunch, which is separated from the next microbunch by the wavelength of the accelerating rf-field or a multiple thereof. The microbunch current or peak current $\hat{I}$ is defined as the total microbunch charge q divided by the microbunch duration τ_μ,

$$\hat{I} = \frac{q}{\tau_\mu} . \tag{11.1}$$

The micro pulse duration must be specially defined to take a nonuniform charge distribution of the particular accelerator into account. A series of microbunches form a beam pulse which is generally determined by the duration of the rf-pulse. In a conventional S-band electron linear accelerator the rf-pulse duration is of the order of a few micro seconds while a superconducting linac can produce a continuous stream of microbunches thus eliminating the pulse structure of the beam. An electrostatic accelerator may produce pulsed beams if the accelerating voltage is applied only for short time intervals. The pulse current I_p is defined as the average

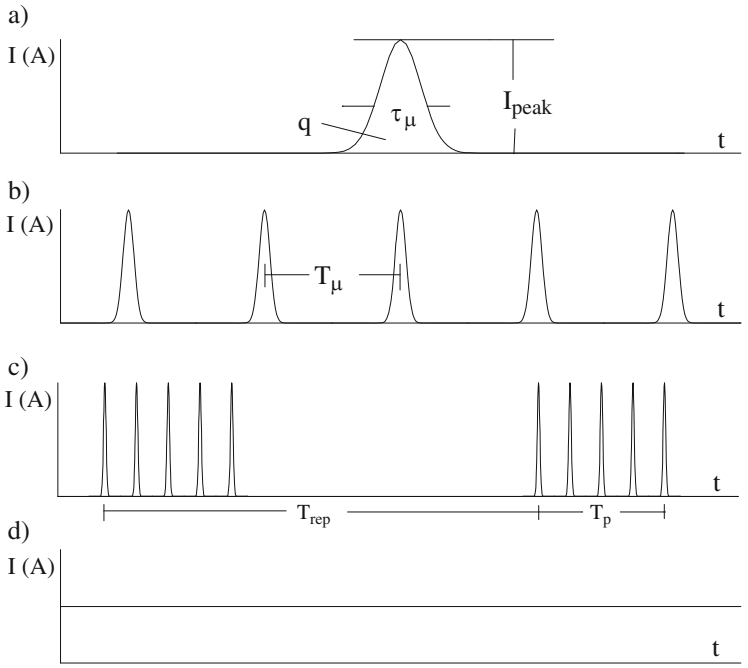

Fig. 11.1 Definitions for time structure and pulse currents. (**a**) Peak current, $\hat{I} = q/\tau_\mu$, where τ_μ is the microbunch duration and q the charge per microbunch. (**b**) Pulse current $I_\mathrm{p} = \hat{I}\,\tau_\mu/T_\mu = q/T_\mu$, where T_μ is the micro-bunch period. (**c**) Average current $\langle I\rangle = I_\mathrm{p} T_\mathrm{p} \nu_\mathrm{rep}$, with T_p the pulse duration and ν_rep the pulse repetition rate. (**d**) Continuous beam current

current during the duration of the pulse. If the duration of the micro bunch is τ_μ and the time between successive microbunches T_μ the pulse current is

$$I_\mathrm{p} = \hat{I}\frac{\tau_\mu}{T_\mu} = \frac{q}{T_\mu}\,. \tag{11.2}$$

The average beam current, finally, is the beam current averaged over a complete cycle of the particular accelerator.

$$\langle I\rangle = I_\mathrm{p}\,\frac{T_\mathrm{p}}{T_\mathrm{r}} = \frac{q}{T_\mathrm{r}}\frac{T_\mathrm{p}}{T_\mu} = \frac{n_\mu\, q}{T_\mathrm{rep}}\,, \tag{11.3}$$

where n_μ is the number of microbunches per pulse and q the charge in a microbunch. In a beam transport line, this is the total charge passing by per unit time, where the unit time is as long as the distance between beam pulses. In a circular accelerator it is, for example, the total circulating charge divided by the revolution time. For the experimenter using particles from a cycling synchrotron accelerator the average current is the total charge delivered to the experiment during a time long compared to the cycling time divided by that time.

The "beam on–beam off" time is measured by the duty factor defined as the fraction of actual beam time to total time at the experimental station. Depending on the application, it is desirable to have a high duty factor where the particles come more uniformly distributed in time compared to a low duty factor where the same number of particles come in short bursts.

11.1.4 Beam Dimensions

Of great importance for the design of particle accelerators is the knowledge of beam size parameters like transverse dimensions, bunch length and energy spread as well as the particle intensity distribution in six-dimensional phase space. In this respect, electron beams may behave different from beams of heavier particles like protons which is a consequence of synchrotron radiation and effects of quantized emission of photons on the dynamic parameters of the electrons. Where such radiation effects are negligible beams of any kind of particles evolve the same way along a beam line. Specifically, we have seen that in such cases the beam emittances are a constant of motion and the beam sizes are therefore modulated only by the variation of the betatron and dispersion functions as determined by the focusing structure. The particle distribution stays constant while rotating in phase space. This is true for the transverse as well as for the longitudinal and energy parameters.

A linear variation of beam emittance with energy is introduced when particles are accelerated or decelerated. We call this variation adiabatic damping, where the beam emittance scales inversely proportional with the particle momentum and the transverse beam size, divergence, bunch length and energy spread scale inversely to the square root of the particle momentum. This adiabatic damping actually is not a true damping process where the area in phase space is reduced. It rather reflects the particular definition of beam emittance with respect to the canonical dimensions of phase space. In transverse beam dynamics we are concerned with geometric parameters and a phase space element would be expressed by the product $\Delta u\, \Delta u'$. Liouville's theorem, however, requires the use of canonical variables, momentum and position, and the same phase space element is $\Delta u\, \Delta p_u$, where $\Delta p_u = p_0 u'$ and u is any of the three degrees of freedom. Acceleration increases the particle momentum p_0 and as a consequence the geometric emittance $\Delta u\, \Delta u'$ must be reduced to keep the product $\Delta u\, \Delta p_u$ constant. This reduction of the geometric emittance by acceleration is called adiabatic damping and occurs in all three degrees of freedom.

More consistent with Liouville's theorem of constant phase space density is the normalized emittance defined by

$$\epsilon_n = \beta\gamma\epsilon\,, \tag{11.4}$$

where γ is the particle energy in units of the rest energy and $\beta = v/c$. This normalized emittance obviously has the appropriate definition to stay constant under the theorem of Liouville.

It is often difficult and not practical to define a beam emittance for the whole beam. Whenever the beam is fuzzy at the edges it may not make sense to include all particles into the definition of the beam emittance and provide expensive aperture for the fuzzy part of the beam. Relativistic electron beams in circular accelerators are particularly fuzzy due to the quantized emission of synchrotron radiation and as a consequence the particle distribution transforms into a Gaussian distribution. Later, we will discuss the evolution of the beam emittance due to statistical effects in great detail and derive the particle distribution from the Fokker-Planck equation. The electron beam emittance is defined for that part of the beam which is contained within one standard unit of the Gaussian distribution. this is true also for any other parameter which assumes a Gaussian distribution like beam size, divergence, energy spread, phase etc.

The beam emittance for particle beams is primarily defined by the characteristic source parameters and source energy. Given perfect matching between different accelerators and beam lines during subsequent acceleration, this source emittance is reduced inversely proportional to the particle momentum by adiabatic damping and stays constant in terms of normalized emittance. This describes accurately the ideal situation for proton and ion beams, for nonrelativistic electrons and electrons in linear accelerators as long as statistical effects are absent. A variation of the emittance occurs in the presence of statistical effects in the form of collisions with other particles or emission of synchrotron radiation and we will concentrate here in more detail on the evolution of beam emittances in highly relativistic electron beams.

Statistical processes cause a spreading of particles in phase space or a continuous increase of beam emittance. In cases where this diffusion is due to the particle density, the emittance increase may decrease significantly because the scattering occurrence drops to lower and lower values as the particle density decreases. Such a case appears in intra-beam scattering [1–3], where particles within the same bunch collide and exchange energy. Specifically when particles exchange longitudinal momentum into transverse momentum and gain back the lost longitudinal momentum from the accelerating cavities. The beam "heats" up transversely which becomes evident in the increased beam emittance and beam sizes.

Statistical perturbations due to synchrotron radiation, however, lead to truly equilibrium states where the continuous excitation due to quantized emission of photons is compensated by damping. Discussing first the effect of damping will prepare us to combine the results with statistical perturbations leading to an equilibrium state of the beam dimensions.

11.2 Damping

Emission of synchrotron radiation causes the appearance of a reaction force on the emitting particle which must be taken into account to accurately describe particle dynamics. In doing so, we note from the theory of synchrotron radiation that the energy lost into synchrotron radiation is lost through the emission of many photons and we may assume that the energy loss is continuous. Specifically, we assume that single photon emissions occur fast compared to the oscillation period of the particle such that we may treat the effect of the recoil force as an impulse.

In general, we must consider the motion of a particle in all three degrees of freedom or in six-dimensional phase space. The appearance of damping stems from the emission of synchrotron radiation in general, but the physics leading to damping in the longitudinal degree of freedom is different from that in the transverse degrees of freedom. The rate of energy loss into synchrotron radiation depends on the particle energy itself being high at high energies and low at low energies. As a consequence, a particle with a higher than ideal energy will loose more energy to synchrotron radiation than the ideal particle and a particle with lower energy will loose less energy. The combined result is that the energy difference between such three particles has been reduced, an effect that shows up as damping of the beam energy spread. With the damping of the energy spread, we observe also a damping of its conjugate variable, the longitudinal phase or bunch length.

In the transverse plane we note that the emission of a photon leads to a loss of longitudinal as well as transverse momentum since the particle performs betatron oscillations. The total lost momentum is, however, replaced in the cavity only in the longitudinal direction. Consequently, the combined effect of emission of a photon and the replacement of the lost energy in accelerating cavities leads to a net loss of transverse momentum or transverse damping.

Although damping mechanisms are different for transverse and longitudinal degrees of freedom, the total amount of damping is limited and determined by the amount of synchrotron radiation. This correlation of damping decrements in all degrees of freedom was derived first by Robinson [4] for general accelerating fields as long as they are not so strong that they would appreciably affect the particle orbit.

11.2.1 Robinson Criterion

Following Robinson's idea we will derive what is now known as Robinson's damping criterion by observing the change of a six dimensional vector in phase space due to synchrotron radiation and acceleration. The components of this vector are the four transverse coordinates (x, x', y, y'), the energy deviation ΔE, and the longitudinal phase deviation from the synchronous phase $\varphi = \psi - \psi_s$. Consistent with smooth approximation a continuous distribution of synchrotron radiation along the orbit is assumed as well as continuous acceleration to compensate energy losses.

During the short time dt the six-dimensional vector

$$\boldsymbol{u} = \left(x,\, x',\, y,\, y',\, \varphi,\, \delta E\right) \tag{11.5}$$

will change by an amount proportional to dt. We may expand the transformations into a Taylor series keeping only linear terms and express the change of the phase space vector in form of a matrix transformation

$$\Delta\boldsymbol{u} = \boldsymbol{u}_1 - \boldsymbol{u}_0 = \mathrm{d}t\, \mathcal{M}\boldsymbol{u}_0\,. \tag{11.6}$$

From the eigenvalue equation for this transformation matrix,

$$\mathcal{M}\boldsymbol{u}_j = \lambda_j \boldsymbol{u}_j\,,$$

where $\boldsymbol{u}_j$ are the eigenvectors, λ_i the eigenvalues being the roots of the characteristic equation $\det(\mathcal{M} - \lambda\mathcal{I}) = 0$ and $\mathcal{I}$ the unity matrix. From (11.6) we get

$$\boldsymbol{u}_1 = (1 + \mathcal{M}\,\mathrm{d}t)\boldsymbol{u}_0 = (1 + \lambda_j\,\mathrm{d}t)\boldsymbol{u}_0 \approx \boldsymbol{u}_0 \mathrm{e}^{\lambda_j\,\mathrm{d}t}\,. \tag{11.7}$$

Since the eigenvectors must be real the eigenvalues come in conjugate complex pairs

$$\lambda_j = \alpha_i \pm \mathrm{i}\beta_i\,,$$

where $i = 1, 2, 3$ and

$$\sum_{j=1}^{j=6} \lambda_j = 2 \sum_{i=1}^{i=3} \alpha_i\,. \tag{11.8}$$

The quantities α_i cause exponential damping or excitation of the eigenvectors depending on whether they are negative or positive, while the β_i contribute only a frequency shift of the oscillations.

Utilizing the transformation matrix $\mathcal{M}$, we derive expressions for the eigenvalues by evaluating the expression $\frac{\mathrm{d}}{\mathrm{d}\tau} \det(\tau\mathcal{M} - \lambda\mathcal{I})|_{\tau=0}$ in two different ways. With $\mathcal{M} = \lambda_j\mathcal{I}$ we get

$$\frac{\mathrm{d}}{\mathrm{d}\tau} \det\left[(\tau\lambda_i - \lambda)\,\mathcal{I}\right]_{\tau=0} = \frac{\mathrm{d}}{\mathrm{d}\tau} \prod_{j=1}^{j=6} (\tau\lambda_j - \lambda)|_{\tau=0} = -\lambda^5 \sum_{j=1}^{j=6} \lambda_j\,. \tag{11.9}$$

On the other hand, we may execute the differentiation on the determinant directly and get

$$\frac{\mathrm{d}}{\mathrm{d}\tau}\det(\tau\mathcal{M}-\geq\mathcal{I})|_{\tau=0}= \tag{11.10}$$

$$\begin{vmatrix} m_{11} & m_{12} & m_{13} & \cdots \\ \tau m_{21} & \tau m_{22}-\lambda & \tau m_{23} & \cdots \\ \tau m_{31} & \tau m_{32} & \tau m_{33}-\lambda & \cdots \\ \cdots & \cdots & \cdots & \cdots \end{vmatrix}_{\tau=0}$$

$$+\begin{vmatrix} \tau m_{11}-\lambda & \tau m_{12} & \tau m_{13} & \cdots \\ m_{21} & m_{22} & m_{23} & \cdots \\ \tau m_{31} & \tau m_{32} & \tau m_{33}-\lambda & \cdots \\ \cdots & \cdots & \cdots & \cdots \end{vmatrix}_{\tau=0}+\cdots$$

$$=-\lambda^5 m_{11}\cdots-\lambda^5 m_{66}=-\lambda^5\sum_{j=1}^{j=6}m_{jj}\,.$$

Comparing (11.9) and (11.10) we note with (11.8) the relation

$$\sum_{j-1}^{j=6}\lambda_j=\sum_{j-1}^{j=6}m_{jj}=2\sum_{i=1}^{i=3}\alpha_i \tag{11.11}$$

between eigenvalues, matrix elements, and damping decrements. To further identify the damping we must determine the transformation. The elements m_{11}, m_{33}, and m_{55} are all zero because the particle positions (x, y, φ) are not changed by the emission of a photon or by acceleration during the time $\mathrm{d}t$.

$$m_{11}=0 \qquad m_{33}=0 \qquad m_{55}=0\,. \tag{11.12}$$

The slopes, however, will change. Since synchrotron radiation is emitted in the forward direction we have no direct change of the particle trajectory due to the emission process. We ignore at this point the effects of a finite radiation opening angle $\theta=\pm 1/\gamma$ and show in connection with the derivation of the vertical beam emittance that this effect is negligible while determining damping. Acceleration will change the particle direction because the longitudinal momentum is increased while the transverse momentum stays constant (see Fig. 11.2).

As shown in Fig. 11.2, a particle with a total momentum p_0 and a transverse momentum p_{0t} due to betatron oscillation emits a photon of energy ε_γ. This process leads to a loss of momentum of $-\Delta p=\varepsilon_\gamma/\beta$, where $\beta=v/c$ and a loss of transverse momentum. Acceleration will again compensate for this energy loss. During acceleration the momentum is increased by $\Delta p_{\mathrm{rf}}=+(P_{\mathrm{rf}}/c\beta)\,\mathrm{d}t$, where P_{rf} is the rf-power to the beam. The transverse momentum during this acceleration

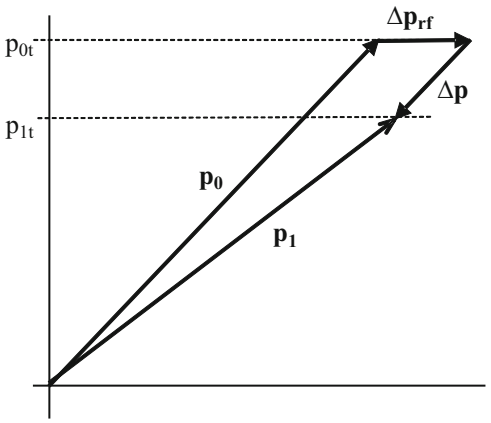

Fig. 11.2 Reduction of the transverse momentum of trajectories by acceleration. For simplicity we assume here that the energy loss $-\Delta p$ due to the emission of a photon is immediately compensated by accelerating fields in a rf-cavity (Δp_{rf})

is not changed and we have therefore $(p_0 - \Delta p)\, u_0' = [p_0 - \Delta p + (P_{\mathrm{rf}}/c\beta)\,\mathrm{d}t]\, u_1'$, where u_0' and u_1' are the slopes of the particle trajectory before and after acceleration, respectively. With $u' = \dot{u}/\beta c$ and $cp_0 = \beta E_0$ we have to first order in Δp and $P_{\mathrm{rf}}\,\mathrm{d}t$

$$\dot{u}_1 = \frac{E_0}{E_0 + P_{\mathrm{rf}}\,\mathrm{d}t}\,\dot{u}_0 \approx \left(1 - \frac{P_{\mathrm{rf}}\,\mathrm{d}t}{E_0}\right)\dot{u}_0\,. \tag{11.13}$$

From (11.7) we get with (11.13) using average values for the synchrotron radiation power around the ring and with $u = x$ or y

$$m_{22} = -\frac{\langle P_\gamma \rangle}{E_0} \quad \text{and} \quad m_{44} = -\frac{\langle P_\gamma \rangle}{E_0}\,, \tag{11.14}$$

where we note that in the absence of acceleration the rf-power is equal to the nominal synchrotron radiation power $\langle P_\gamma \rangle = U_0/T_0$. The energy variation of the particle is the combination of energy loss $-P_\gamma\,\mathrm{d}t$ and gain $P_{\mathrm{rf}}\,\mathrm{d}t$. With

$$P_\gamma(E) = P_\gamma(E_0) + \left.\frac{\partial P_\gamma}{\partial E}\right|_0 \Delta E_0 \quad \text{and} \quad P_{\mathrm{rf}}(\psi) = P_{\mathrm{rf}}(\psi_{\mathrm{s}}) + \left.\frac{\partial P_{\mathrm{rf}}}{\partial \psi}\right|_{\psi_{\mathrm{s}}} \varphi\,,$$

where $\varphi = \psi - \psi_{\mathrm{s}}$ we get

$$\begin{aligned} \Delta E_1 &= \Delta E_0 - \left\langle P_\gamma(E) \right\rangle \mathrm{d}t + P_{\mathrm{rf}}(\psi)\,\mathrm{d}t \\ &= \Delta E_0 - \left.\frac{\partial \left\langle P_\gamma \right\rangle}{\partial E}\right|_0 \Delta E\,\mathrm{d}t + \left.\frac{\partial P_{rf}}{\partial \psi}\right|_{\psi_{\mathrm{s}}} \varphi\,\mathrm{d}t \end{aligned} \tag{11.15}$$

because $P_\gamma(E_0) = P_{\mathrm{rf}}(\psi_\mathrm{s})$. Equation (11.15) exhibits two more elements of the transformation matrix

$$m_{65} = \left.\frac{\partial P_{\mathrm{rf}}}{\partial \psi}\right|_{\psi_\mathrm{s}} \quad \text{and} \quad m_{66} = -\left.\frac{\partial \langle P_\gamma \rangle}{\partial E}\right|_0 . \tag{11.16}$$

We have now all elements necessary to determine the damping decrements. From (11.12), (11.14), (11.16) we get the sum of the damping decrements

$$\sum_{i=1}^{i=3} \alpha_i = \tfrac{1}{2} \sum_{j=1}^{j=6} m_{jj} = -\frac{\langle P_\gamma \rangle}{E_0} - \tfrac{1}{2} \left.\frac{\partial \langle P_\gamma \rangle}{\partial E}\right|_0 , \tag{11.17}$$

which depends only on the synchrotron radiation power and the particle energy. This result was first derived by Robinson [4] and is known as Robinson's damping criterion.

We may separate the damping decrements. For a plane circular accelerator without vertical bending magnets and coupling, the vertical damping decrement $\alpha_y = \alpha_2$ can be extracted. Since the vertical motion is not coupled to either the horizontal or the synchrotron oscillations, we get from (11.14) and (11.17)

$$\alpha_y = -\tfrac{1}{2} \frac{\langle P_\gamma \rangle}{E_0} . \tag{11.18}$$

The damping decrement for synchrotron oscillations has been derived in (9.27) and is

$$\alpha_z = -\tfrac{1}{2} \left.\frac{\mathrm{d}\langle P_\gamma \rangle}{\mathrm{d}E}\right|_0 . \tag{11.19}$$

The horizontal damping decrement finally can be derived from Robinson's damping criterion (11.17) and the two known decrements (11.18), (11.19) to be

$$\alpha_x = -\tfrac{1}{2} \frac{\langle P_\gamma \rangle}{E_0} - \tfrac{1}{2} \left.\frac{\partial \langle P_\gamma \rangle}{\partial E}\right|_0 + \tfrac{1}{2} \left.\frac{\mathrm{d}\langle P_\gamma \rangle}{\mathrm{d}E}\right|_0 . \tag{11.20}$$

We may further evaluate the total and partial differential of the synchrotron radiation power P_γ with energy E. The synchrotron radiation power is proportional to the square of the particle energy E and magnetic field B at the source of radiation and the partial differential is therefore

$$\left.\frac{\partial P_\gamma}{\partial E}\right|_0 = 2 \frac{\langle P_\gamma \rangle}{E_0} . \tag{11.21}$$

The total differential of the synchrotron radiation power depends not only on the particle energy directly but also on the variation of the magnetic field with energy as seen by the particle. A change in the particle energy causes a shift in the particle orbit where the η-function is nonzero and this shift may move the particle to a location with different field strength. To include all energy dependent contributions, we inspect the definition of the average synchrotron radiation power $\langle P_\gamma \rangle = \frac{1}{T_0} \oint P_\gamma \mathrm{d}\tau$ and noting that for highly relativistic particles $c\mathrm{d}\tau = \mathrm{d}z = \left(1 + \frac{\eta}{\rho}\frac{\Delta E}{E_0}\right)\mathrm{d}z$ the average radiation power becomes

$$\langle P_\gamma \rangle = \frac{1}{cT_0} \oint P_\gamma \left(1 + \frac{\eta}{\rho}\frac{\Delta E}{E_0}\right) \mathrm{d}z. \tag{11.22}$$

Differentiating (11.22) with respect to the energy

$$\left.\frac{\mathrm{d}\langle P_\gamma \rangle}{\mathrm{d}E}\right|_0 = \frac{1}{cT_0} \oint \left[\left.\frac{\mathrm{d}P_\gamma}{\mathrm{d}E}\right|_0 + P_\gamma \frac{\eta}{\rho E_0} \right] \mathrm{d}z\,, \tag{11.23}$$

where

$$\left.\frac{\mathrm{d}P_\gamma}{\mathrm{d}E}\right|_0 = 2\,\frac{P_\gamma}{E_0} + 2\,\frac{P_\gamma}{B_0}\,\frac{\mathrm{d}B}{\mathrm{d}x}\,\frac{\mathrm{d}x}{\mathrm{d}E} = 2\,\frac{P_\gamma}{E_0} + 2\,\frac{P_\gamma}{E_0}\rho\, k\, \eta\,.$$

Collecting all components, the synchrotron oscillation damping decrement (11.19) is finally

$$\alpha_z = -\tfrac{1}{2}\left.\frac{\mathrm{d}\langle P_\gamma \rangle}{\mathrm{d}E}\right|_0 = -\tfrac{1}{2}\frac{\langle P_\gamma \rangle}{E_0}\,(2 + \vartheta)\,, \tag{11.24}$$

where we used $\langle P_\gamma \rangle \propto \oint \kappa^2 \mathrm{d}z$ and $P_{\gamma 0} \propto \kappa^2$ with $\kappa = 1/\rho$

$$\vartheta = \frac{\oint \kappa^3 \eta \left(1 + 2\rho^2 k\right)\, \mathrm{d}z}{\oint \kappa^2 \mathrm{d}z}\,. \tag{11.25}$$

Similarly, we get from (11.20) for the horizontal damping decrement

$$\alpha_x = -\frac{1}{2}\frac{\langle P_\gamma \rangle}{E_0}\,(1 - \vartheta)\,. \tag{11.26}$$

In summary the damping decrements for betatron and synchrotron oscillations can be expressed by

$$\begin{aligned}
\alpha_z &= -\frac{1}{2}\frac{\langle P_\gamma \rangle}{E}(2+\vartheta) = -\frac{1}{2}\frac{\langle P_\gamma \rangle}{E} J_z\,, \\
\alpha_x &= -\frac{1}{2}\frac{\langle P_\gamma \rangle}{E}(1-\vartheta) = -\frac{1}{2}\frac{\langle P_\gamma \rangle}{E} J_x\,, \\
\alpha_y &= -\frac{1}{2}\frac{\langle P_\gamma \rangle}{E} \qquad\quad = -\frac{1}{2}\frac{\langle P_\gamma \rangle}{E} J_y\,,
\end{aligned} \tag{11.27}$$

where the factors J_i are the damping partition numbers,

$$\begin{aligned}
J_z &= 2+\vartheta, \\
J_x &= 1-\vartheta, \\
J_y &= 1.
\end{aligned} \tag{11.28}$$

Robinson's damping criterion can be expressed by

$$\sum_i J_i = 4\,. \tag{11.29}$$

In more practical quantities, the damping decrements can be obtained with (24.35) from

$$\alpha_u = -\tfrac{1}{3} r_\mathrm{e} c\, \gamma^3 \left\langle \frac{1}{\rho^2} \right\rangle J_u. \tag{11.30}$$

Damping occurs in circular electron accelerators in all degrees of freedom. In transverse planes particles oscillate in the potential created by quadrupole focusing and any finite amplitude is damped by synchrotron radiation damping. Similarly, longitudinal synchrotron oscillations are contained by a potential well created by the rf-fields and the momentum compaction and finite deviations of particles in energy and phase are damped by synchrotron radiation damping. We note that the synchrotron oscillation damping is twice as strong as transverse damping.

All oscillation amplitudes a_u in six dimensional phase space are damped ($\alpha < 0$) or anti-damped ($\alpha > 0$) like

$$a_u = a_{0u} \mathrm{e}^{\alpha_u t} \tag{11.31}$$

and the damping or rise times are

$$\tau_u = \frac{1}{a_u}. \tag{11.32}$$

In a particular choice of lattice, damping rates can be shifted between different degrees of freedom and special care must be exercised when combined function magnets or strong sector magnets are introduced into a ring lattice.

Both the synchrotron and betatron oscillation damping can be modified by a particular choice of lattice. From (11.25) we note the contribution $\kappa^3\eta$ which is caused by sector magnets. Particles with higher energies follow a longer path in a sector magnet and therefore radiate more. Consequently synchrotron damping is increased with ϑ. This term vanishes for rectangular magnets and must be modified appropriately for wedge magnets. For a rectangular magnet

$$\vartheta_{\text{rect}} = \frac{\oint 2\kappa\eta k \,\mathrm{d}z}{\oint \kappa^2 \mathrm{d}z} \tag{11.33}$$

and for wedge magnets

$$\vartheta_{\text{wedge}} = \frac{\sum_i \left[\kappa^2\theta_0\eta_0 + \int 2(\kappa\eta k)\,\mathrm{d}z + \kappa^2\theta_\mathrm{e}\eta_\mathrm{e}\right]_i}{\oint \kappa^2 \mathrm{d}z}, \tag{11.34}$$

where we add all contributions from all magnets i in the ring. The edge angles at the entrance θ_0 and exit θ_e are defined to be positive going from a rectangular magnet toward a sector magnet.

The second term in the nominator of (11.25) becomes significant for combined function magnets and vanishes for separated function magnets. Specifically. a strong focusing gradient ($k > 0$) combined with beam deflection can contribute significantly to ϑ. For $\vartheta = 1$ all damping in the horizontal plane is lost and anti-damping or excitation of betatron oscillations appears for $\vartheta > 1$. This occurs, for example, in older combined function synchrotrons. At low energies, however, the beam in such lattices is still stable due to strong adiabatic damping and only at higher energies when synchrotron radiation reduces acceleration will horizontal anti-damping take over and dictate an upper limit to the feasibility of such accelerators. Conversely, vertical focusing ($k < 0$) can be implemented into bending magnets such that the horizontal damping is actually increased since $\vartheta < 0$. However, there is a limit for the stability of synchrotron oscillations for $\vartheta = 2$.

11.3 Particle Distribution in Longitudinal Phase Space

The particle distribution in phase space is rarely uniform. To determine the required aperture in a particle transport system avoiding excessive losses we must, however, know the particle distribution. Proton and ion beams involve particle distributions which due to Liouville's theorem do not change along a beam transport system, except for the variation of the betatron and dispersion function. The particle distribution can therefore be determined by measurements of beam transmission

through a slit for varying openings. If this is done at two points about 90° apart in betatron phase space, angular as well as spatial distribution can be determined.

This procedure can be applied also to electrons in a transport system. The distribution changes, however, significantly when electrons are injected into a circular accelerator. We will discuss the physics behind this violation of Liouville's theorem and determine the resulting electron distribution in phase space.

Relativistic electron and positron beams passing through bending magnets emit synchrotron radiation, a process that leads to quantum excitation and damping. As a result the original beam emittance at the source is completely replaced by an equilibrium emittance that is unrelated to the original source characteristics. Postponing a rigorous treatment of statistical effects to Chap. 12 we concentrate here on a more visual discussion of the reaction of synchrotron radiation on particle and beam parameters.

11.3.1 Energy Spread

Statistical emission of photons causes primarily a change of particle energy leading to an energy spread within the beam. To evaluate the effect of quantized emission of photons on the beam energy spread, we observe particles undergoing synchrotron oscillations so that a particle with an energy deviation A_0 at time t_0 will have an energy error at time t of

$$A\,(t) = A_0\,\mathrm{e}^{\mathrm{i}\Omega(t-t_0)} \tag{11.35}$$

Emission of a photon with energy ε at time t_1 causes a perturbation and the particle continues to undergo synchrotron oscillations but with a new amplitude

$$A_1 = A_0\mathrm{e}^{\mathrm{i}\Omega(t-t_0)} - \varepsilon\,\mathrm{e}^{\mathrm{i}\Omega(t-t_1)} \tag{11.36}$$

The change in oscillation amplitude due to the emission of one photon of energy ε can be derived from (11.36) by multiplying with its imaginary conjugate for

$$A_1^2 = A_0^2 + \varepsilon^2 - 2\varepsilon A_0 \cos\left[\Omega\,(t_1 - t_0)\right]. \tag{11.37}$$

Because the times at which photon emission occurs is random we have for the average increase in oscillation amplitude due to the emission of a photon of energy ε

$$\left\langle \Delta A^2 \right\rangle = \left\langle A_1^2 - A_0^2 \right\rangle = \varepsilon^2 \tag{11.38}$$

The rate of change in amplitude per unit time due to this statistical or quantum excitation while averaging around the ring is

$$\left\langle \left.\frac{\mathrm{d}A^2}{\mathrm{d}t}\right|_{\mathrm{q}} \right\rangle_z = \int_0^\infty \varepsilon^2 \dot{n}\,(\varepsilon)\;\mathrm{d}\epsilon = \left\langle \dot{\mathcal{N}}_{\mathrm{ph}} \left\langle \varepsilon^2 \right\rangle \right\rangle_z \tag{11.39}$$

where $\dot{n}(\varepsilon)$ is the number of photons of energy ε emitted per unit time and energy bin $\mathrm{d}\varepsilon$. This can be equated to the total photon flux $\dot{\mathcal{N}}_{\mathrm{ph}}$ multiplied by the average square of the photon energy and again taking the average along the orbit.

Damping causes a reduction in the synchrotron oscillation amplitude and with $A = A_0 \mathrm{e}^{\alpha_s t}$ and the synchrotron oscillation damping time $\tau_z = 1/|\alpha_z|$ (11.27)

$$\left\langle \left. \frac{\mathrm{d}A^2}{\mathrm{d}t} \right|_{\mathrm{d}} \right\rangle_z = -\frac{2}{\tau_z} \left\langle A^2 \right\rangle . \tag{11.40}$$

Both quantum excitation and damping lead to an equilibrium state

$$\left\langle \dot{\mathcal{N}}_{\mathrm{ph}} \left\langle \varepsilon^2 \right\rangle \right\rangle_z - \frac{2}{\tau_z} \left\langle A^2 \right\rangle = 0, \tag{11.41}$$

or solving for $\left\langle A^2 \right\rangle$

$$\left\langle A^2 \right\rangle = \tfrac{1}{2} \tau_z \left\langle \dot{\mathcal{N}}_{\mathrm{ph}} \left\langle \varepsilon^2 \right\rangle \right\rangle_z . \tag{11.42}$$

Due to the central limit theorem of statistics the energy distribution caused by the statistical emission of photons assumes a Gaussian distribution with the standard root mean square energy spread $\sigma_\varepsilon^2 = \frac{1}{2} \left\langle A^2 \right\rangle$. The photon spectrum will be derived in Part 22.6 and the integral in (11.39) can be evaluated to give [5]

$$\dot{\mathcal{N}}_{\mathrm{ph}} \left\langle \varepsilon^2 \right\rangle = \frac{55}{24\sqrt{3}} P_\gamma \varepsilon_{\mathrm{c}} \tag{11.43}$$

Replacing the synchrotron radiation power P_γ by its expression in (24.34) and the critical photon energy $\varepsilon_{\mathrm{c}} = \hbar \omega_{\mathrm{c}}$ by (24.49) we get

$$\dot{\mathcal{N}}_{\mathrm{ph}} \left\langle \varepsilon^2 \right\rangle = \frac{55}{32\pi\sqrt{3}} \left[c C_\gamma \hbar c \left(mc^2 \right)^4 \gamma^7 \kappa^3 \right] \tag{11.44}$$

with $C_\gamma = \frac{4\pi}{3} \frac{r_{\mathrm{e}}}{\left(mc^2\right)^3} = 8.8460 \times 10^{-5}$ m/GeV^{3}and the equilibrium energy spreadbecomes finally with (11.27) and (24.34)

$$\frac{\sigma_\varepsilon^2}{E^2} = \frac{\tau_z}{4E^2} \left\langle \dot{\mathcal{N}}_{\mathrm{ph}} \left\langle \varepsilon^2 \right\rangle \right\rangle_z = C_{\mathrm{q}} \frac{\gamma^2}{J_z} \frac{\left\langle \kappa^3 \right\rangle_z}{\left\langle \kappa^2 \right\rangle_z} \tag{11.45}$$

where

$$C_{\mathrm{q}} = \frac{55}{32\sqrt{3}} \frac{\hbar c}{mc^2} = 3.84 \times 10^{-13} \text{ m} \tag{11.46}$$

for electrons and positrons. The equilibrium energy spread in an electron storage ring depends only on the beam energy and the bending radius.

11.3.2 Bunch Length

The conjugate coordinate to the energy deviation is the phase and a spread of particle energy appears also as a spread in phase or as a longitudinal particle distribution and an equilibrium bunch length. The bunch length is

$$\sigma_\ell = \frac{c|\eta_c|}{\Omega}\frac{\sigma_\varepsilon}{E_0} \tag{11.47}$$

and replacing the synchrotron oscillation frequency by its expression (9.35) we get finally for the equilibrium bunch length in a circular electron accelerator

$$\sigma_\ell = \frac{\sqrt{2\pi}c}{\omega_{\mathrm{rev}}}\sqrt{\frac{\eta_c E_0}{he\hat{V}\cos\psi_s}}\frac{\sigma_\varepsilon}{E_0}. \tag{11.48}$$

The equilibrium electron bunch length can be varied by varying the rf-voltage and scales like $\sigma_\ell \propto 1/\sqrt{\hat{V}}$ which is a much stronger dependence than the scaling obtained for non-radiating particles in Sect. 9.3.5. A very small bunch length can be obtained by adjusting the momentum compaction to a small value including zero. As the momentum compaction approaches zero, but second order terms must be considered which has been discussed in detail in Sect. 9.4.4. An electron storage ring where the momentum compaction is adjusted to be zero or close to zero is called an isochronous ring [6] or a quasi isochronous ring [7]. Such rings do not yet exist at this time but are intensely studied and problems are being solved in view of great benefits for research in high energy physics, synchrotron radiation sources and free electron lasers to produce short particle or light pulses.

11.4 Transverse Beam Emittance

The sudden change of particles energy due to the quantized emission of photons also causes a change in the characteristics of transverse particle motion. Neither position nor the direction of the particle trajectory is changed during the forward emission of photons. From beam dynamics, however, we know that different reference trajectories exist for particles with different energies. Two particles with energies cp_1 and cp_2 follow two different reference trajectories separated at the position z along the beam transport line by a distance

$$\Delta x\,(z) = \eta(z)\,\frac{cp_1 - cp_2}{cp_0}\,, \tag{11.49}$$

where $\eta(z)$ is the dispersion function and cp_0 the reference energy. Although particles in general do not exactly follow these reference trajectories, they do

perform betatron oscillations about these trajectories. The sudden change of the particle energy causes a sudden change in the reference path and thereby a sudden change in the betatron oscillation amplitude.

11.4.1 Equilibrium Beam Emittance

Postponing again a rigorous discussion of the evolution of phase space due to statistical perturbations to the next chapter, we follow here a more intuitive path to determine the equilibrium transverse beam emittance. Similar to the discussion leading to the equilibrium energy spread we will observe perturbations to the transverse motion caused by photon emission. In the case of longitudinal quantum excitation it was sufficient to consider the effect of photon emission on the particle energy alone since the particle phase is not changed by this process.

As a particle emits a photon it will not change its actual position and direction. However, the position of a particle with respect to the ideal reference orbit is the combination of its betatron oscillation amplitude and a chromatic contribution due to a finite energy deviation and dispersion. Variation of the particle position $u = u_\beta + \eta\,(\Delta E/E_0)$, and direction $u' = u'_\beta + \eta'\,(\Delta E/E_0)$ due ε is described by

$$\begin{aligned} \delta u = 0 = \delta u_\beta + \eta\tfrac{\epsilon}{E} \quad &\text{or } \delta u_\beta = -\eta\tfrac{\epsilon}{E}, \\ \delta u' = 0 = \delta u'_\beta + \eta'\tfrac{\epsilon}{E} \quad &\text{or } \delta u'_\beta = -\eta'\tfrac{\epsilon}{E}. \end{aligned} \tag{11.50}$$

We note the sudden changes in the betatron amplitudes and slopes because the sudden energy loss leads to a simultaneous change in the reference orbit. This perturbation will modify the phase ellipse the particles move on. The variation of the phase ellipse $\gamma u^2 + 2\alpha u u' + \beta {u'}^2 = a^2$ is expressed by

$$\gamma\delta(u_\beta^2) + 2\alpha\delta(u_\beta u'_\beta) + \beta\delta({u'_\beta}^2) = \delta(a^2)$$

and inserting the relations (11.50) we get terms of the form $\delta(u_\beta^2) = (u_{\beta 0} + \delta u_\beta)^2 - u_{\beta 0}^2$ etc. Emission of photons can occur at any betatron phase and we therefore average over all phases. As a consequence, all terms depending linearly on the betatron amplitude and its derivatives or variations thereof vanish. The average variation of the phase ellipse or oscillation amplitude a due to the emission of photons with energy ε becomes then

$$\langle \delta a^2 \rangle = \frac{\varepsilon^2}{E_0^2}\mathcal{H}(z)\,, \tag{11.51}$$

where

$$\mathcal{H}(z) = \beta\eta'^2 + 2\alpha\eta\,\eta' + \gamma\eta^2\,. \tag{11.52}$$

We average again over all photon energies, multiply by the total number of photons emitted per unit time and integrate over the whole ring to get the variation of the oscillation amplitude per turn

$$\Delta\langle a^2\rangle = \frac{1}{c\,E_0^2}\oint \dot{N}_{\mathrm{ph}}\langle\varepsilon^2\rangle\mathcal{H}(z)\,\mathrm{d}z\,. \tag{11.53}$$

The rate of change of the oscillation amplitude is then with $z = ct$

$$\left.\frac{\mathrm{d}\langle a^2\rangle}{\mathrm{d}t}\right|_{\mathrm{q}} = \frac{1}{E_0^2}\left\langle\dot{N}_{\mathrm{ph}}\langle\varepsilon^2\rangle\mathcal{H}(z)\right\rangle_z\,, \tag{11.54}$$

where the index z indicates averaging around the ring. This quantum excitation of the oscillation amplitude is compensated by damping for which we have similar to (11.40)

$$\left\langle\frac{\mathrm{d}a^2}{\mathrm{d}t}\right\rangle\bigg|_{\mathrm{d}} = 2\alpha_x\langle a^2\rangle\,. \tag{11.55}$$

Equilibrium is reached when quantum excitation and damping are of equal strength which occurs for

$$\frac{\sigma_u^2}{\beta_u} = \frac{\tau_u}{4E^2}\left\langle\dot{N}_{\mathrm{ph}}\langle\varepsilon^2\rangle\mathcal{H}_u\right\rangle_z\,. \tag{11.56}$$

Here we have used the definition of the standard width of a Gaussian particle distribution

$$\sigma_u^2 = \langle u^2(z)\rangle = \left\langle\tfrac{1}{2}a^2\beta_u\right\rangle \tag{11.57}$$

with the betatron function β_u and $u = x$ or y. With (11.27), (11.44) and (24.34) we get finally

$$\epsilon_u = \frac{\sigma_u^2}{\beta_u} = C_{\mathrm{q}}\frac{\gamma^2}{J_u}\frac{\langle\kappa^3\mathcal{H}_u\rangle}{\langle\kappa^2\rangle}\,, \tag{11.58}$$

which we define as the equilibrium beam emittance of a relativistic electron in a circular accelerator.

11.4.2 Emittance Increase in a Beam Transport Line

In (11.53) we decided to integrate the quantum excitation over a complete turn of a circular accelerator. This should not be taken as a restriction but rather as an example. If we integrate along an open beam transport line we would get the increase of the beam emittance along this beam line. This becomes important for very high energy linear colliders where beams are transported along the linear accelerator and some beam transport system in the final focus section just ahead of the collision point. Any dipole field along the beam path contributes to an increase of the beam emittance, whether it be real dipole magnets, dipole field errors, path displacements in a quadrupole, or small correction magnets for beam steering. Since there is no damping, the emittance growth is therefore in both planes from (11.53) and (11.57)

$$\Delta\epsilon_u = \frac{1}{2cE_0^2}\int \dot{N}_{\mathrm{ph}}\langle\varepsilon^2\rangle\mathcal{H}_u(z)\,\mathrm{d}z\,. \tag{11.59}$$

The function $\mathcal{H}$ is now evaluated with the dispersion functions $D_u(z)$ instead of the periodic η-function with contributions from any dipole field. Since such fields can occur in both planes there is an emittance increase in both planes as well. With (11.44) the increase in beam emittance is finally

$$\Delta\epsilon_u = \frac{55C_\gamma\hbar c(mc^2)^2}{64\pi\sqrt{3}}\gamma^5\int \kappa^3\mathcal{H}_u\,\mathrm{d}z\,, \tag{11.60}$$

where the integration is taken along the beam line. The perturbation of the beam emittance in a beam transport line increases with the fifth power of the particle energy. At very high energies we expect therefore a significant effect of dipole errors on the beam emittance even if the basic beam transport line is straight.

So far, we have not yet distinguished between the horizontal and vertical plane since the evolution of the phase space does not depend on the particular degree of freedom. The equilibrium beam emittance, however, depends on machine parameters and circular accelerators are not constructed symmetrically. Specifically, accelerators are mostly constructed in a plane and therefore there is no deflection in the plane normal to the ring plane. Assuming bending only occurs in the horizontal plane, we may use (11.58) directly as the result for the horizontal beam emittance $u = x$ only.

11.4.3 Vertical Beam Emittance

In the vertical plane, the bending radius $\rho_v \to \infty$ and the vertical beam emittance reduces to zero by virtue of damping. Whenever we have ideal conditions like this it is prudent to consider effects that we may have neglected leading to less than ideal

results. In this case, we have neglected the fact that synchrotron radiation photons are emitted not strictly in the forward direction but rather into a small angle $\pm 1/\gamma$. Photons emitted at a slight angle exert a recoil on the particle normal to the direction of the trajectory. A photon emitted at an angle θ with respect to the direction of the trajectory and an azimuth ϕ causes a variation of the vertical slope by

$$\delta y' = -\theta \cos\phi \frac{\varepsilon}{E_0},$$

while the position is not changed $\delta y = 0$. This leads to a finite beam emittance which can be derived analogous to the general derivation above

$$\frac{\sigma_y^2}{\beta_y} = \frac{\tau_y}{4E^2} \left\langle \dot{N}_{\mathrm{ph}} \langle \varepsilon^2 \theta^2 \cos^2\phi \rangle \beta_y \right\rangle_z . \tag{11.61}$$

We set

$$\langle \varepsilon^2 \theta^2 \cos^2\phi \rangle \approx \langle \varepsilon^2 \rangle \left\langle \theta^2 \right\rangle \left\langle \cos^2\phi \right\rangle \approx \langle \varepsilon^2 \rangle \frac{1}{2\gamma^2}$$

and get finally for the fundamental lower limit of the vertical beam emittance

$$\frac{\sigma_y^2}{\beta_y} = \epsilon_y = C_{\mathrm{q}} \frac{\overline{\beta}_y}{2J_y} \frac{\langle \kappa^3 \rangle}{\langle \kappa^2 \rangle} . \tag{11.62}$$

Very roughly $\epsilon_y/\epsilon_x = 1/\gamma^2 \ll 1$ and it is therefore justified to neglect this term in the calculation of the horizontal beam emittance. This fundamental lower limit of the equilibrium beam emittance is of the order of 10^{-13} m, assuming the betatron function and the bending radius to be of similar magnitude, and therefore indeed very small compared to actual achieved beam emittances in real accelerators. In reality, we observe a larger beam emittance in the vertical plane due to coupling or due to vertical steering errors which create a small vertical dispersion and, consequently, a small yet finite vertical beam emittance. As a practical rule the vertical beam emittance is of the order of one percent or less of the horizontal beam emittance due to field and alignment tolerances of the accelerator magnets. For very small horizontal beam emittances, however, this percentage may increase because the vertical beam emittance due to vertical dipole errors becomes more significant.

Sometimes it is necessary to include vertical bending magnets in an otherwise horizontal ring. In this case the vertical dispersion function is finite and so is $\mathcal{H}_y(z)$. The vertical emittance is determined by evaluating (11.58) while using the vertical dispersion function. Note, however, that all bending magnets must be included in the calculation of equilibrium beam emittances because for quantum excitation it is immaterial whether the energy loss was caused in a horizontally or vertically bending magnet. The same is true for the damping term in the denominator. Differences in the horizontal and vertical beam emittance come from the different betatron and η-functions at the location of the radiation source.

11.4.4 Beam Sizes

Beam parameters like width, height, length, divergence, and energy spread are not all fixed independent quantities, but rather depend on emittances and lattice and rf-parameters. These multiple dependencies allow the adjustment of beam parameters, within limits, to be optimum for the intended application. In this section we will discuss such dependencies.

A particle beam at any point of a beam transport line may be represented by a few phase ellipses for different particle momenta as shown in Fig. 11.3. The phase ellipses for different momenta are shifted proportional to the dispersion function at that point and its derivative. Generally, the form and orientation of the ellipses are slightly different too due to chromatic aberrations in the focusing properties of the beam line. For the definition of beam parameters we need therefore the knowledge of the lattice functions including chromatic aberrations and the beam emittance and momentum spread.

The particle beam width or beam height is determined by the emittance, betatron function, dispersion function and energy spread. The betatron and dispersion functions vary along a beam transport line and depend on the distribution of the beam focusing elements. The beam sizes are therefore also functions of the location along the beam line. From the focusing lattice these functions can be derived and the beam sizes be calculated.

The beam size of a particle beam is generally not well defined since the boundaries of a beam tends to be fuzzy. We may be interested in the beam size that defines all of a particle beam. In this case we look for that phase ellipse that

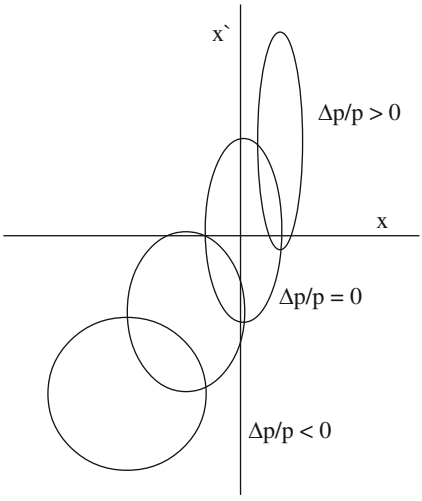

Fig. 11.3 Distribution of beam ellipses for a beam with finite emittance and momentum spread (schematic). The variation in the shape of the phase ellipses for different energies reflect the effect of chromatic aberrations

encloses all particles and obtain the beam size in the form of the beam envelope. The beam half-width or half-height of this beam envelope is defined by

$$u_\beta(z) = \sqrt{\epsilon_u \beta_u(z)} \tag{11.63}$$

with $u = (x, y)$. If there is also a finite momentum spread within the beam particles the overall beam size or beam envelope is increased by the dispersion

$$u_\eta(z) = \eta_u(z) \frac{\Delta cp}{cp_0} \tag{11.64}$$

and the total beam size is

$$u_{\text{tot}}(z) = u_\beta(z) + u_\eta(z) = \sqrt{\epsilon_u \beta_u(z)} + \eta_u(z) \frac{\Delta cp}{cp_0}. \tag{11.65}$$

This definition of the beam size assumes a uniform particle distribution within the beam and is used mostly to determine the acceptance of a beam transport system. The acceptance of a beam transport system is defined as the maximum emittance a beam may have and still pass through the vacuum chambers of a beam line. In Fig. 11.3 this would be the area of that ellipse that encloses the whole beam including off momentum particles. In practice, however, we would choose a larger acceptance to allow for errors in the beam path.

Since the lattice functions vary along a beam line the required aperture to let a beam with the maximum allowable emittance pass is not the same everywhere along the system. To characterize the aperture variation consistent with the acceptance, a beam stay clear area, BSC, is defined as the required material free aperture of the beam line.

The beam parameters for a Gaussian particle distributions are defined as the standard values of the Gaussian distribution $\sigma_x, \sigma_{x'}, \sigma_y, \sigma_{y'}, \sigma_\delta, \sigma_\ell$,where most designations have been defined and used in previous chapters and where $\sigma_\delta = \sigma_\epsilon / cp_0$ and σ_ℓ the bunch length. Quoting beam sizes for any particle type in units of σ can be misleading specifically in connection with beam intensities. For example, a beam with a horizontal and vertical size of one sigma has a cross section of $2\sigma_x 2\sigma_y$ and includes only 46.59 % of the beam. This is accepted for electron beams with Gaussian distribution but for proton beams intensities are often given for $\sqrt{6}\sigma$'s to cover most of the beam. In Table 11.1 the fraction of the total beam intensity is compiled for a few generally used units of beam size measurement and for beam size, cross section, and volume. The beam size for Gaussian beams is thereby

$$\sigma_{\text{u,tot}} = \sqrt{\epsilon_u \beta_u(z) + \eta^2(z)\sigma_\delta^2}\,. \tag{11.66}$$

Four parameters are required to determine the beam size in each plane although in most cases the vertical dispersion vanishes.

Table 11.1 Fraction of total beam intensity

	One-dimension (%)	Two-dimension (%)	Three-dimension (%)
1σ	68.26	46.59	31.81
2σ	95.44	91.09	86.93
$\sqrt{6}\sigma$	98.56	97.14	95.74

11.4.5 Beam Divergence

The angular distribution of particles within a beam depends on the rotation of the phase ellipse and we define analogous to the beam size an angular beam envelope by

$$\sigma_{\mathrm{u}',\mathrm{tot}} = \sqrt{\epsilon_u \gamma_u(z) + \eta'^2(z)\,\sigma_\delta^2}\,. \tag{11.67}$$

Again, there is a contribution from the betatron motion, from a finite momentum spread and from associated chromatic aberration. The horizontal and vertical beam divergencies are also determined by four parameters in each plane.

11.5 Variation of the Damping Distribution

Robinson's criterion provides an expression for the overall damping in six-dimensional phase space without specifying the distribution of damping in the three degrees of freedom. In accelerators we make an effort to decouple the particle motion in the three degrees of freedom as much as possible and as a result we try to optimize the beam parameters in each plane separately from the other planes for our application. Part of this optimization is the adjustment of damping and as a consequence of beam emittances to desired values. Robinson's criterion allows us to modify the damping in one plane at the expense of damping in another plane. This shifting of damping is done by varying damping partition numbers.

From the definition of the ϑ parameter is clear that damping partition numbers can be modified depending on whether the accelerator lattice is a combined function or a separated function lattice. Furthermore, we may adjust virtually any distribution between partition numbers by choosing a combination of gradient and separated function magnets.

11.5.1 Damping Partition and Rf-Frequency

Actually such "gradients" can be introduced even in a separated function lattice. If the rf-frequency is varied the beam will follow a path that meets the synchronicity condition. Increasing the rf-frequency, for example, leads to a shorter wavelength

and therefore the total path length in the ring need to be shorter. As a consequence of the principle of phase stability the beam energy is reduced and the beam follows a lower energy equilibrium orbit with the same harmonic number as the reference orbit for the reference energy. Decreasing the rf-frequency leads just to the opposite effect. The off momentum orbits pass systematically off center through quadrupoles which therefore function like combined function gradient magnets.

To quantify this effect we use only the second term in the expression (11.25) for ϑ. The first term, coming from sector magnets, will stay unaffected. Displacement of the orbit in the quadrupoles will cause a bending with a bending radius

$$\frac{1}{\rho_\mathrm{q}} = k\,\delta x\,. \tag{11.68}$$

An rf-frequency shift causes a momentum change of

$$\frac{\Delta p}{p_0} = -\frac{1}{\alpha_\mathrm{c}}\frac{\Delta f_\mathrm{rf}}{f_\mathrm{rf}}\,, \tag{11.69}$$

which in turn causes a shift in the equilibrium orbit of

$$\delta x = \eta\frac{\Delta p}{p_0} = -\frac{\eta}{\alpha_\mathrm{c}}\frac{\Delta f_\mathrm{rf}}{f_\mathrm{rf}} \tag{11.70}$$

and the bending radius of the shifted orbit in quadrupoles is

$$\frac{1}{\rho_\mathrm{q}} = k\delta x = k\eta\frac{\Delta p}{p_0} = -k\frac{\eta}{\alpha_\mathrm{c}}\frac{\Delta f_\mathrm{rf}}{f_\mathrm{rf}}\,. \tag{11.71}$$

Inserted into the second term of (11.25), we get

$$\Delta\vartheta = -\frac{1}{\alpha_\mathrm{c}}\frac{\oint 2k^2\eta^2\,\mathrm{d}z}{\oint\frac{1}{\rho_0^2}\mathrm{d}z}\frac{\Delta f_\mathrm{rf}}{f_\mathrm{rf}}\,, \tag{11.72}$$

where ρ_0 is the bending radius of the ring bending magnets All quantities in (11.72) are fixed properties of the lattice and changing the rf-frequency leads just to the expected effect. Specifically, we note that all quadrupoles contribute additive irrespective of their polarity. We may apply this to a simple isomagnetic FODO lattice where all bending magnets and quadrupoles have the same absolute strength respectively with $\oint \mathrm{d}z/\rho_0^2 = 2\pi/\rho_0$. Integration of the nominator in (11.72) leads to

$$\oint 2\,k^2\eta^2\mathrm{d}z = 2\,k^2(\eta_\mathrm{max}^2 + \eta_\mathrm{min}^2)l_\mathrm{q}2\,n_\mathrm{c}\,,$$

where l_q is half the quadrupole length in a FODO lattice, η_max and η_min the values of the η-function in the focusing QF and defocusing QD quadrupoles, respectively,

and n_c the number of FODO cells in the ring. With all this the variation of the ϑ parameter

$$\Delta\vartheta = -n_c \frac{2\,\rho_0}{\pi\,\alpha_c l_q} \frac{\eta_{max}^2 + \eta_{min}^2}{f^2} \frac{\Delta f_{rf}}{f_{rf}} . \tag{11.73}$$

Here we have used the focal length $f^{-1} = k\,l_q$. Replacing in (11.73) the η functions by the expressions (10.74) derived for a FODO lattice, we recall the relation $f = \kappa\,L$ and get finally [8]

$$\Delta\vartheta = -\frac{\rho_0}{\rho} \frac{1}{\alpha_c} \frac{L}{l_q} (4\kappa^2 + 1) \frac{\Delta f_{rf}}{f_{rf}} , \tag{11.74}$$

where ρ is the average bending radius in the FODO cell. The variation of the ϑ parameter in a FODO lattice is the more sensitive to rf-frequency variations the longer the cell compared to the quadrupole length and the weaker the focusing. For other lattices the expressions may not be as simple as for the FODO lattice but can always be computed numerically by integrations and evaluation of (11.72).

By varying the rf-frequency and thereby the horizontal and longitudinal damping partition number we have found a way to either increase or decrease the horizontal beam emittance. The adjustments, however, are limited. To decrease the horizontal beam emittance we would increase the horizontal partition number and at the same time the longitudinal partition number would be reduced. The limit is reached when the longitudinal motion becomes unstable or in practical cases when the partition number drops below about half a unit. Other more practical limits may occur before stability limits are reached if, for example, the momentum change becomes too large to fit the beam into the vacuum chamber aperture.

11.6 Variation of the Equilibrium Beam Emittance

In circular electron accelerators the beam emittance is determined by the emission of synchrotron radiation and the resulting emittance is not always equal to the desired value. In such situations methods to alter the equilibrium emittance are desired and we will discuss in the next sections such methods which may be used to either increase or decrease the beam emittance.

11.6.1 Beam Emittance and Wiggler Magnets

The beam emittance in an electron storage ring can be greatly modified by the use of wiggler magnets both to increase [9] or to decrease the beam emittance. A decrease in beam emittance has been noted by Tazzari [10] while studying the effect of a

number of wiggler magnets in a low emittance storage ring design. Manipulation of the beam emittance in electron storage rings has become of great interest to obtain extremely small beam emittances and we will therefore derive systematic scaling laws for the effect of wiggler magnets on the beam emittance as well as on the beam energy spread [10, 11].

The particle beam emittance in a storage ring is the result of two competing effects, the quantum excitation caused by the quantized emission of photons and the damping effect. Both effects lead to an equilibrium beam emittance observed in electron storage rings.

Independent of the value of the equilibrium beam emittance in a particular storage ring, it can be further reduced by increasing the damping without also increasing the quantum excitation. More damping can be established by causing additional synchrotron radiation through the installation of deflecting dipole magnets like strong wigglers magnets. In order to avoid quantum excitation of the beam emittance, however, the placement of wiggler magnets has to be chosen carefully. As discussed earlier, an increase of the beam emittance through quantum excitation is caused only when synchrotron radiation is emitted at a place in the storage ring where the dispersion function is finite. Emittance reducing wiggler magnets therefore must be placed in areas around the storage ring where the dispersion vanishes to minimize quantum excitation. To calculate the modified equilibrium beam emittance, we start from (11.54) and get with (11.44) and (11.57) an expression for the quantum excitation of the emittance which can be expanded to include wiggler magnets

$$\left.\frac{\mathrm{d}\epsilon}{\mathrm{d}t}\right|_{\mathrm{q},0} = \frac{2}{3} r_\mathrm{e} C_\mathrm{q} \gamma^5 \left\langle \kappa^3 \mathcal{H} \right\rangle_0 , \tag{11.75}$$

The quantity $\mathcal{H}$ is evaluated for the plane for which the emittance is to be determined, E is the particle energy, and ρ the bending radius of the regular ring magnets. The average $\langle\rangle$ is to be taken for the whole ring and the index $_0$ indicates that the average $\left\langle \kappa^3 \mathcal{H} \right\rangle_0$ be taken only for the ring proper without wiggler magnets.

Since the contributions of different magnets, specifically, of regular storage ring magnets and wiggler magnets are independent of each other, we may use the results of the basic ring lattice and add to the regular quantum excitation and damping the appropriate additions due to the wiggler magnets,

$$\left.\frac{\mathrm{d}\epsilon}{\mathrm{d}t}\right|_{\mathrm{q,w}} = \frac{2}{3} r_\mathrm{e} C_\mathrm{q} \gamma^5 \left[\left\langle \kappa^3 \mathcal{H} \right\rangle_0 + \left\langle \kappa^3 \mathcal{H} \right\rangle_\mathrm{w} \right] . \tag{11.76}$$

Both, ring magnets and wiggler magnets produce synchrotron radiation and contribute to damping of the transverse particle oscillations. Again, we may consider both contributions separately and adding the averages we get the combined rate of emittance damping from (11.55) and (11.27)

$$\left.\frac{\mathrm{d}\epsilon}{\mathrm{d}t}\right|_{\mathrm{d,w}} = -\frac{2}{3} r_\mathrm{e} c \epsilon_\mathrm{w} J_u \gamma^3 \left[\left\langle \kappa^2 \right\rangle_0 + \left\langle \kappa^2 \right\rangle_\mathrm{w} \right] , \tag{11.77}$$

where ϵ_w is the beam emittance with wiggler magnets and J_u the damping partition number with $u = x, y$. The equilibrium beam emittance is reached when the quantum excitation rate and the damping rates are of equal magnitude. We add therefore (11.76) and (11.77) and solve for the emittance

$$\epsilon_\mathrm{w} = C_\mathrm{q} \frac{\gamma^2}{J_x} \frac{\langle \kappa^3 \mathcal{H} \rangle_0 + \langle \kappa^3 \mathcal{H} \rangle_\mathrm{w}}{\langle \kappa^2 \rangle_0 + \langle \kappa^2 \rangle_\mathrm{w}} . \tag{11.78}$$

With ϵ_0 being the unperturbed beam emittance the relative emittance change due to the presence of wiggler magnets is

$$\frac{\epsilon_\mathrm{w}}{\epsilon_0} = \frac{1 + \langle \kappa^3 \mathcal{H} \rangle_\mathrm{w} / \langle \kappa^3 \mathcal{H} \rangle_0}{1 + \langle \kappa^2 \rangle_\mathrm{w} / \langle \kappa^2 \rangle_0} . \tag{11.79}$$

Making use of the definition of average parameter values we get with the circumference of the storage ring $C = 2\pi R$

$$\begin{aligned} \langle \kappa^3 \mathcal{H} \rangle_0 &= \tfrac{1}{C} \oint |\kappa_0^3| \, \mathcal{H} \mathrm{d}z , & \langle \kappa^3 \mathcal{H} \rangle_\mathrm{w} &= \tfrac{1}{C} \oint |\kappa_\mathrm{w}^3| \, \mathcal{H} \mathrm{d}z , \\ \langle \kappa^2 \rangle_0 &= \tfrac{1}{C} \oint \kappa_0^2 \mathrm{d}z , & \text{and} \quad \langle \kappa^2 \rangle_\mathrm{w} &= \tfrac{1}{C} \oint \kappa_\mathrm{w}^2 \mathrm{d}z . \end{aligned} \tag{11.80}$$

Evaluation of these integrals for the particular storage ring and wiggler magnet employed gives from (11.79) the relative change in the equilibrium beam emittance. We note that the quantum excitation term scales like the cube while the damping scales only quadratically with the wiggler curvature. This feature leads to the effect that the beam emittance is always reduced for small wiggler fields and increases only when the third power terms become significant.

Concurrent with a change in the beam emittance a change in the momentum spread due to the wiggler radiation can be derived similarly,

$$\frac{\sigma_{\epsilon\mathrm{w}}^2}{\sigma_{\epsilon 0}^2} = \frac{1 + \langle \kappa^3 \rangle_\mathrm{w} / \langle \kappa^3 \rangle_0}{1 + \langle \kappa^2 \rangle_\mathrm{w} / \langle \kappa^2 \rangle_0} . \tag{11.81}$$

Closer inspection of (11.79) and (11.81) reveals basic rules and conditions for the manipulations of beam emittance and energy spread. If the ring dispersion function is finite in the wiggler section strong quantum excitation may occur depending on the magnitude of the wiggler magnet bending radius ρ_w. This situation is desired if the beam emittance must be increased [9]. If wiggler magnets are placed into a storage ring lattice were the ring dispersion function vanishes, only the small dispersion function due to the wiggler magnets must be considered for the calculation of $\langle \mathcal{H}_\mathrm{w} \rangle$ and therefore only little quantum excitation occurs. In this case the beam emittance can be reduced since the wiggler radiation contributes more strongly to damping and we call such magnets damping wigglers [10, 11]. Whenever wiggler magnets are used which are stronger than the ordinary ring magnets $\rho_\mathrm{w} < \rho_0$ the momentum spread in the beam is increased. This is true for virtually all cases of interest.

Conceptual methods to reduce the beam emittance in a storage ring have been derived which are based on increased synchrotron radiation damping while avoiding quantum excitation effects. Optimum lattice parameters necessary to achieve this will be derived in the next section.

11.6.2 Damping Wigglers

The general effects of wiggler magnet radiation on the beam emittance has been described and we found that the beam emittance can be reduced if the wiggler is placed where $\eta = 0$ to eliminate quantum excitation. This assumption, however, is not quite correct. Even though we have chosen a place, where the storage ring dispersion function vanishes, the quantum excitation factor $\mathcal{H}_\mathrm{w}$ is not exactly zero once the wiggler magnets are turned on because they create their own dispersion function. To calculate this dispersion function, we assume a sinusoidal wiggler field [11]

$$B(z) = B_\mathrm{w} \cos k_\mathrm{p} z \,, \tag{11.82}$$

where $k_\mathrm{p} = 2\pi/\lambda_\mathrm{p}$ and λ_p the wiggler period length (Fig. 11.4). The differential equation for the dispersion function is then

$$\eta'' = \kappa = \kappa_\mathrm{w} \cos k_\mathrm{p} z \,, \tag{11.83}$$

which can be solved by

$$\begin{aligned} \eta(z) &= \tfrac{\kappa_\mathrm{w}}{k_\mathrm{p}^2} \left(1 - \cos k_\mathrm{p} z\right) \,, \\ \eta'(z) &= \tfrac{\kappa_\mathrm{w}}{k_\mathrm{p}} \sin k_\mathrm{p} z \,, \end{aligned} \tag{11.84}$$

where we have assumed that the wiggler magnet is placed in a dispersion free location $\eta_0 = \eta_0' = 0$. With this solution, the first two Eqs. (11.80) can be evaluated. To simplify the formalism we ignore the z-dependence of the lattice functions within the wiggler magnet setting $\alpha_x = 0$ and $\beta_x = \text{const}$. Evaluating the integrals (11.80), we note that the absolute value of the bending radius must be used along the integration path because the synchrotron radiation does not depend on the sign of the deflection. With this in mind, we evaluate the integrals $\int_0^{\lambda_\mathrm{p}/2} \left|\kappa^3\right| \eta^2 \, \mathrm{d}z$

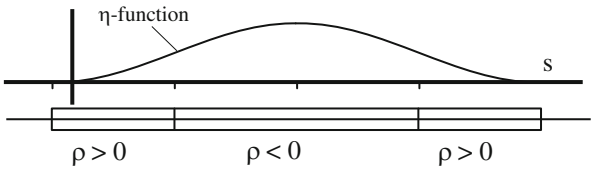

Fig. 11.4 Dispersion function in one period of a wiggler magnet

and $\int_0^{\lambda_p/2} \left|\kappa^3\right| \eta'^2 \, \mathrm{d}z$. For each half period of the wiggler magnet the contribution to the integral is

$$\Delta \int_0^{\lambda_p/2} \left|\kappa^3\right| \mathcal{H} \, \mathrm{d}z = \frac{12}{5} \frac{1}{\beta_x} \frac{\kappa_w^5}{k_p^5} + \frac{4}{15} \frac{\kappa_w^5 \beta_x}{k_p^3} \approx \frac{4}{15} \frac{\kappa_w^5 \beta_x}{k_p^3} , \tag{11.85}$$

where the approximation $\lambda_p \ll \beta_x$ was used. For the whole wiggler magnet with N_w periods the total quantum excitation integral is with the deflection angle per wiggler half pole $\Theta_w = \kappa_w / k_p$

$$\int_w \left|\kappa_w^3\right| \mathcal{H} \, \mathrm{d}z \approx N_w \frac{8}{15} \frac{\beta_x}{\rho_w^2} \Theta_w^3 . \tag{11.86}$$

Similarly, the damping integral for the total wiggler magnet is

$$\int_w \kappa^2 \, \mathrm{d}z = \pi \, N_w \, \kappa_w \Theta_w . \tag{11.87}$$

Inserting expressions (11.80), (11.86), (11.87) into (11.79), we get for the emittance ratio

$$\frac{\epsilon_{xw}}{\epsilon_{x0}} = \frac{1 + \frac{4}{15\pi} N_w \frac{\beta_x}{\langle \mathcal{H}_0 \rangle} \frac{\rho_0^2}{\rho_w^2} \Theta_w^3}{1 + \frac{1}{2} N_w \frac{\rho_0}{\rho_w} \Theta_w} , \tag{11.88}$$

where $\langle \mathcal{H}_0 \rangle$ is the average value of $\mathcal{H}$ in the ring bending magnets excluding the wiggler magnets. We note from (11.88) that the beam emittance indeed can be reduced by wiggler magnets if Θ_w is kept small. For easier numerical calculation we replace $\langle \mathcal{H}_0 \rangle$ by the unperturbed beam emittance which is in the limit $\rho_w \to \infty$

$$\langle \mathcal{H}_0 \rangle = \frac{J_x \rho_0 \epsilon_{x0}}{C_q \gamma^2} \tag{11.89}$$

and get instead of (11.88)

$$\frac{\epsilon_{xw}}{\epsilon_{x0}} = \frac{1 + \frac{4\, C_q}{15\pi J_x} N_w \frac{\beta_x}{\epsilon_{x0}\, \rho_w} \gamma^2 \frac{\rho_0}{\rho_w} \Theta_w^3}{1 + \frac{1}{2} N_w \frac{\rho_0}{\rho_w} \Theta_w} . \tag{11.90}$$

The beam emittance is reduced by wiggler magnets whenever the condition

$$\frac{8}{15\pi} \frac{C_q}{J_x} \frac{\beta_x}{\epsilon_0 \, \rho_w} \gamma^2 \Theta_w^2 \leq 1 \tag{11.91}$$

is fulfilled. For large numbers of wiggler poles $N_\mathrm{w} \to \infty$ the beam emittance reaches asymptotically a lower limit given by

$$\epsilon_{x\mathrm{w}} \to \frac{8}{15\pi} \frac{C_\mathrm{q}}{J_x} \frac{\beta_x}{\rho_\mathrm{w}} \gamma^2 \Theta_\mathrm{w}^2 \,. \tag{11.92}$$

In this limit the ultimate beam emittance is independent of the unperturbed beam emittance. This derivation did not include any perturbation of the original lattice functions due to focusing effects by the wiggler poles. Such perturbations are either small or must be compensated such that our assumptions still are valid.

For many wiggler poles the increase in momentum spread also reaches an asymptotic limit which is given from (11.81)

$$\frac{\sigma_{\epsilon\mathrm{w}}^2}{\sigma_{\epsilon o}^2} \to \frac{\rho_0}{\rho_\mathrm{w}} = \frac{B_\mathrm{w}}{B_0} \,, \tag{11.93}$$

where B_0 is the magnetic field strength in the ring magnets. Beam stability and acceptance problems may occur if the beam momentum spread is allowed to increase too much and therefore inclusion of damping wigglers must be planned with some caution.

11.7 Robinson Wiggler*

The horizontal betatron motion in a combined function synchrotron FODO lattice is not damped because $\vartheta > 1$. Beam stability in a synchrotron therefore exists only during acceleration when the anti-damping is over compensated by adiabatic damping, and the maximum energy achievable in a combined function synchrotron is determined when the quantum excitation becomes too large to be compensated by adiabatic damping. In an attempt, at the Cambridge Electron Accelerator CEA, to convert the synchrotron into a storage ring the problem of horizontal beam instability was solved by the proposal [12] to insert a damping wiggler consisting of a series of poles with alternating fields and gradients designed such that the horizontal partition number becomes positive and $-2 < \vartheta < 1$.

Such magnets can be used generally to vary the damping partition numbers without having to vary the rf-frequency and thereby moving the beam away from the center of the beam line.

11.7.1 Damping Partition and Synchrotron Oscillation

The damping partition number and damping depend on the relative momentum spread of the whole beam. During synchrotron oscillations, significant momentum deviations can occur, specifically, in the tails of a Gaussian distribution. Such

momentum deviations, although only temporary, can lead to reduced damping or outright anti-damping [8]. To quantify this effect, we write (11.72) in the form

$$\Delta\vartheta = \frac{\oint 2\,k^2\eta^2\,\mathrm{d}z}{\oint \kappa_a^2 \mathrm{d}z}\frac{\Delta p}{p_0} = C_0\frac{\Delta p}{p_0}. \tag{11.94}$$

The momentum deviation is not a constant but rather oscillates with the synchrotron oscillation frequency,

$$\frac{\Delta p}{p_0} = \left.\frac{\Delta p}{p_0}\right|_{\max} \sin\Omega t = \delta_{\max}\sin\Omega t\,, \tag{11.95}$$

where Ω is the synchrotron oscillation frequency. The damping partition number oscillates as well (11.94) and the damping decrement is therefore

$$\frac{1}{\tau} = \frac{1}{\tau_{x0}}(1 - C_0\delta_{\max}\sin\Omega t)\,. \tag{11.96}$$

If the perturbation is too large we have anti-damping during part of the synchrotron oscillation period. As a consequence the beam is "breathing" in its horizontal and longitudinal dimensions while undergoing synchrotron oscillations. To quantify this, we calculate similar to (11.56) the total rate of change of the betatron oscillation amplitude a^2, as defined by the phase space ellipse $\gamma u^2 + 2\alpha uu' + \beta u'^2 = a^2$, composed of quantum excitation and modified damping

$$\frac{\mathrm{d}\langle a^2\rangle}{\mathrm{d}t} = \frac{\langle \dot{N}_{\mathrm{ph}}\langle\epsilon_\gamma^2\rangle\mathcal{H}\rangle}{E_0^2} - \frac{2\langle a^2\rangle}{\tau}\,. \tag{11.97}$$

The amplitude a^2 has the dimension of an emittance but we are interested here in the maximum amplitude which can be expressed in terms of a betatron amplitude by $a^2 = u_{\max}^2/\beta_u$. Replacing the varying damping time by $\tau^{-1} = \tau_0^{-1}(1 - \delta_{\max}C_0\sin\Omega t)$ (11.97) becomes

$$\frac{\mathrm{d}\langle u_{\max}^2\rangle}{\langle u_{\max}^2\rangle} = \frac{2}{\tau_0}\,\delta_{\max}C_0\sin\Omega t\,\mathrm{d}t\,,$$

which can be readily integrated to give

$$\langle u_{\max}^2\rangle = \langle u_{\max,0}^2\rangle\exp\left[\frac{2\,\delta_{\max}C_0}{\Omega\,\tau_0}(1-\cos\Omega t)\right]. \tag{11.98}$$

A particle with a betatron amplitude $u_{\max,0}$ will, during the course of a synchrotron oscillation period, reach amplitudes as large as $u_{\max}$. The effect is the largest for particles with large energy oscillations. On the other hand, the effect on the core of the beam is generally very small since $\delta_{\max}$ is small.

11.7.2 Can We Eliminate the Beam Energy Spread?

To conclude the discussions on beam manipulation we try to conceive a way to eliminate the energy spread in a particle beam. From beam dynamics we know that the beam particles can be sorted according to their energy by introducing a dispersion function. The distance of a particle from the reference axis is proportional to its energy and given by

$$x_\delta = D\delta\,, \tag{11.99}$$

where D is the value of the dispersion at the location under consideration and $\delta = \Delta E/E_0$ the energy error. For simplicity we make no difference between energy and momentum during this discussion. We consider now a cavity excited at a higher mode such that the accelerating field is zero along the axis, but varies linearly with the distance from the axis. If now the accelerating field, or after integration through the cavity, the accelerating voltage off axis is

$$eV_{\mathrm{rf}}(x_\delta) = -\frac{x_\delta}{D}E_0\,, \tag{11.100}$$

we have just compensated the energy spread in the beam. The particle beam has become monochromatic, at least to the accuracy assumed here. In reality the dispersion of the beam is not perfect due to the finite beam emittance.

We will discuss cavity modes and find that the desired mode exists indeed and the lowest order of such modes is the TM_{110}-mode. So far we seem to have made no mistake and yet, Liouville's theorem seems to be violated because this scheme does not change the bunch length and the longitudinal emittance has been indeed reduced by application of macroscopic fields.

The problem is that we are by now used to consider transverse and longitudinal phase space separate. While this separation is desirable to manage the mathematics of beam dynamics, we must not forget, that ultimately beam dynamics occurs in six-dimensional phase space. Since Liouville's theorem must be true, its apparent violation warns us to observe changes in other phase space dimensions. In the case of beam monochromatization we notice that the transverse beam emittance has been increased. The transverse variation of the longitudinal electric field causes by virtue of Maxwell's equations the appearance of transverse magnetic fields which deflect the particles transversely thus increasing the transverse phase space at the expense of the longitudinal phase space.

This is a general feature of electromagnetic fields which is known as the Panofsky-Wenzel theorem [13] stating that transverse acceleration occurs whenever there is a transverse variation of the longitudinal accelerating field. We will discuss this in more detail in Sect. 22.1.4. So, indeed we may monochromatize a particle beam with the use of a TM_{110}-mode, but only at the expense of an increase in the transverse beam emittance.

11.8 Beam Life Time

Particles travelling along a beam transport line or orbiting in a circular accelerator can be lost due to a variety of causes. We ignore the trivial cases of beam loss due to technical malfunctioning of beam line components or losses caused by either complete physical obstruction of the beam line or a mismatch of vacuum chamber aperture and beam dimensions. For a well designed beam transport line or circular accelerator we distinguish two main classes for particle loss which are losses due to scattering and losses due to instabilities. While particle losses due to scattering with other particles is a single particle effect leading to a gradual loss of beam intensity, instabilities can lead to catastrophic loss of part or all of the beam. In this chapter we will concentrate on single particle losses due to interactions with residual gas atoms.

The effect of particle scattering on the beam parameters is different in a beam transport line compared to a circular accelerator especially compared to storage rings. Since a beam passes through transport lines only once, we are not concerned about beam life time but rather with the effect of particle scattering on the transverse beam size. For storage rings, in contrast, we consider both the effect of scattering on the beam emittance as well as the overall effect on the beam lifetime. Since long lifetimes of the order of many hours are desired in storage rings even small effects can accumulate to reduce beam performance significantly. In proton rings continuous scattering with residual gas atoms or with other protons of the same beam can change the beam parameters considerably for lack of damping. Even for electron beams, where we expect the effects of scattering to vanish within a few damping times, we may observe an increase in beam emittance. This is specifically true due to intra beam scattering for dense low emittance beams at low energies when damping is weak.

Collisions of particles with components of residual gas atoms, losses due to a finite acceptance limited by the physical or dynamic aperture, collisions with other particles of the same beam, or with synchrotron radiation photons can lead to absorption of the scattered particles or cause large deflections leading to instable trajectories and eventual particle loss. The continuous loss of single particles leads to a finite beam lifetime and may in severe cases require significant hardware modifications or a different mode of operation to restore a reasonable beam lifetime.

Each of these loss mechanisms has a particular parameter characterizing and determining the severity of the losses. Scattering effects with residual gas atoms are clearly dominated by the vacuum pressure while scattering effects with other particles in the same beam depend on the particle density. Some absorption of particles at the vacuum chamber walls will always occur due to the Gaussian distribution of particles in space. Even for non-radiating proton beams which are initially confined to a small cross section, we observe the development of a halo of particles outside the beam proper due to intra beam scattering. The expansion of this halo is obviously limited by the vacuum chamber aperture. In circular accelerators this aperture limitation may not only be effected by solid vacuum chambers but also by "soft walls" due to stability limits imposed by the dynamic aperture.

Longitudinal phase or energy oscillations are limited either by the available rf-parameters determining the momentum acceptance or by the transverse acceptance at locations, where the dispersion function is nonzero whichever is more restrictive. A momentum deviation or spread translates at such locations into a widening of the beam and particle loss occurs if the momentum error is too large to fit within the stable aperture. Transverse oscillation amplitudes are limited by the transverse acceptance as limited by the vacuum chamber wall or by aberrations due to nonlinear fields.

11.8.1 Beam Lifetime and Vacuum

Particle beams are generally confined within evacuated chambers to avoid excessive scattering on residual gas atoms. Considering multiple Coulomb scattering alone the rms radial scattering angle of particles with momentum p and velocity β passing through a scattering material of thickness L can be described by [14, 15]

$$\vartheta_{\mathrm{rms}} = Z \frac{20_{\mathrm{MeV}}}{\beta cp} \sqrt{\frac{L}{L_{\mathrm{r}}}}\,, \tag{11.101}$$

where Z is the charge multiplicity of the particle and L_{r} the radiation length of the scattering material. We may integrate (11.101) and get the beam radius r of a pencil beam after passing through a scatterer of thickness L

$$r \approx Z \frac{40_{\mathrm{MeV}} L}{3\beta cp} \sqrt{\frac{L}{L_{\mathrm{r}}}}\,. \tag{11.102}$$

The beam emittance generated by scattering effects is then in both the horizontal and vertical plane just the product of the projections of the distance r of the particles from the reference path and the radial scattering angles ϑ onto the respective plane. From (11.101), (11.102) the beam emittance growth due to Coulomb scattering in a scatterer of length L is then

$$\epsilon_{x,y}(\mathrm{rad\,m}) = Z^2 \frac{2}{3} \left(\frac{14(\mathrm{MeV})}{\beta cp} \right)^2 \frac{L^2(\mathrm{m})}{L_{\mathrm{r}}(\mathrm{m})}\,. \tag{11.103}$$

For atmospheric air the radiation length is $L_{\mathrm{r}} = 300.5$ m and a pencil electron beam with a momentum of say $cp = 1{,}000\,\mathrm{MeV}$ passing through 20 m of atmospheric air would grow through scattering to a beam diameter of 6.9 cm or to a beam emittance of about 177 mrad mm in each plane. This is much too big an increase in beam size to be practical in a 20 m beam transport line let alone in a circular accelerator or storage ring, where particles are expected to circulate at nearly the speed of light for many turns like in a synchrotron or for many hours in a storage ring.

To avoid beam blow up due to scattering we obviously need to provide an evacuated environment to the beam with a residual gas pressure which must be the lower the longer the beam is supposed to survive scattering effects. This does not mean that beam transport in atmospheric pressure must be avoided at all cost. Sometimes it is very useful to let a beam pass though air to provide free access for special beam monitoring devices specifically at the end of a beam transport line before the beam is injected into a circular accelerator. Obviously, this can be done only if the scattering effects through very thin metallic windows and the short length of atmospheric air will not spoil the beam emittance too much.

Elastic Scattering

As particles travel along an evacuated pipe they occasionally collide with atoms of the residual gas. These collisions can be either on nuclei or electrons of the residual gas atoms. The physical nature of the collision depends on the mass of the colliding partners. Particles heavier than electrons suffer mostly an energy loss in collisions with the atomic shell electrons while they lose little or no energy during collisions with massive nuclei but are merely deflected from their path by elastic scattering. The lighter electrons in contrast suffer both deflection as well as energy losses during collisions.

In this section we concentrate on the elastic scattering process, where the energy of the fast particle is not changed. For the purpose of calculating particle beam lifetimes due to elastic or Coulomb scattering we ignore screening effects by shell electrons and mathematical divergence problems at very small scattering angles. The scattering process therefore is described by the classical Rutherford scattering with the differential cross section per atom

$$\frac{\mathrm{d}\sigma}{\mathrm{d}\Omega} = \frac{1}{4\pi\epsilon_0}\left(\frac{zZe^2}{2\beta cp}\right)^2 \frac{1}{\sin^4(\theta/2)}\,, \tag{11.104}$$

where z is the charge multiplicity of the incident particle eZ the charge of the heavy scattering nucleus, θ the scattering angle with respect to the incident path, Ω the solid angle with $\mathrm{d}\Omega = \sin\theta\,\mathrm{d}\theta\,\mathrm{d}\varphi$, and φ the polar angle.

To determine the particle beam lifetime or the particle loss rate we will calculate the rate of events for scattering angles larger than a maximum value of $\hat{\theta}$ which is limited by the acceptance of the beam transport line. Any particle being deflected by an angle larger than this maximum scattering angle will be lost. We integrate the scattering cross section over all angles greater than $\hat{\theta}$ up to the maximum scattering angle π. With n scattering centers or atoms per unit volume and N beam particles the loss rate is

$$-\frac{\mathrm{d}N}{\mathrm{d}t} = 2\pi c\beta nN \int_{\hat{\theta}}^{\pi} \frac{\mathrm{d}\sigma}{\mathrm{d}\Omega}\sin\theta\,\mathrm{d}\theta\,. \tag{11.105}$$

Under normal conditions at 0 °C and a gas pressure of 760 mm mercury the number of scattering centers in a homogeneous gas is equal to twice Avogadro's number $\mathcal{A}$ and becomes for an arbitrary gas pressure P

$$n = 2\mathcal{A}\frac{P(\text{Torr})}{760} = 2 \times 2.68675 \times 10^{19}\frac{P(\text{Torr})}{760}\,. \tag{11.106}$$

The factor 2 comes from the fact that homogeneous gases are composed of two atomic molecules, where each atom acts as a separate scattering center. This assumption would not be true for single atomic noble gases which we do not consider here, but will be included in a later generalization. The integral on the r.h.s. of (11.105) becomes with (11.104)

$$\int_{\hat{\theta}}^{\pi} \frac{\sin\theta\,\mathrm{d}\theta}{\sin^4(\theta/2)} = \frac{2}{\tan^2(\hat{\theta}/2)}\,. \tag{11.107}$$

Dividing (11.105) by N we find an exponential decay of beam intensity with time

$$N = N_0 \mathrm{e}^{-t/\tau}\,, \tag{11.108}$$

where the decay time constant or beam lifetime is

$$\tau^{-1} = c\beta 2\mathcal{A}\frac{P(\text{Torr})}{760}\left(\frac{zZe^2}{2\beta cp}\right)^2 \frac{4\pi}{\tan^2(\hat{\theta}/2)}\,. \tag{11.109}$$

The maximum acceptable scattering angle $\hat{\theta}$ is limited by the acceptance ϵ_A of the beam transport line. A particle being scattered by an angle θ at a location where the betatron function has the value β_θ reaches a maximum betatron oscillation amplitude of $a = \sqrt{\beta_a \beta_\theta}\,\theta$ elsewhere along the beam transport line where the betatron function is β_a. The minimum value of A^2/β_A along the ring lattice, where A is the vacuum chamber aperture or the limit of the dynamic aperture whichever is smaller, is equal to the ring acceptance

$$\epsilon_A = \left.\frac{A^2}{\beta_A}\right|_{\min}\,. \tag{11.110}$$

For simplicity we ignore here the variation of the betatron function and take an average value $\langle\beta\rangle$ at the location of the scattering event and get finally for the maximum allowable scattering angle

$$\hat{\theta}^2 = \frac{\epsilon_A}{\langle\beta\rangle}\,. \tag{11.111}$$

This angle is generally rather small and we may set $\tan(\hat{\theta}/2) \approx (\hat{\theta}/2)$. Utilizing these definitions and approximations we obtain for the lifetime of a beam made up

of singly charged particles $z = 1$ due to elastic Coulomb scattering expressed in more practical units

$$\tau_{\rm cs}\,(\text{hours}) = 10.25\,\frac{(cp)^2\,\left(\text{GeV}^2\right)\,\epsilon_{\rm A}\,(\text{mm mrad})}{\langle\beta\,(\text{m})\rangle\,P\,(\text{nTorr})}\,, \tag{11.112}$$

where we have assumed that the residual gas composition is equivalent to nitrogen gas N_2 with $Z^2 \approx 49$. The Coulomb scattering lifetime is proportional to the ring acceptance or proportional to the square of the aperture A where A^2/β is a minimum.

The particle loss due to Coulomb scattering is most severe at low energies and increases with the acceptance of the beam transport line. Furthermore, the beam lifetime depends on the focusing in the transport line through the average value of the betatron function. If instead of averaging the betatron function we integrate the contributions to the beam lifetime along the transport line we find that the effect of the scattering event depends on the betatron function at the location of the collision and the probability that such a collision occurs at this location depends on the gas pressure there. Therefore, it is prudent to not only minimize the magnitude of the betatron functions alone but rather minimize the product βP along the transport line. Specifically, where large values of the betatron function cannot be avoided, extra pumping capacity should be provided to reach locally a low vacuum pressure for long Coulomb scattering lifetime.

We have made several simplifications and approximations by assuming a homogeneous gas and assuming that the maximum scattering angle be the same in all directions. In practical situations, however, the acceptance need not be the same in the vertical and horizontal plane. First we will derive the beam lifetime for non-isotropic aperture limits. We assume that the apertures in the horizontal and vertical plane allow maximum scattering angles of $\hat{\theta}_x$ and $\hat{\theta}_y$. Particles are then lost if the scattering angle θ into a polar angle φ exceeds the limits

$$\theta > \frac{\hat{\theta}_x}{\cos\varphi} \quad \text{and} \quad \theta > \frac{\hat{\theta}_y}{\sin\varphi}\,. \tag{11.113}$$

The horizontal aperture will be relevant for all particles scattered into a polar angle between zero and $\arctan(\hat{\theta}_y/\hat{\theta}_x)$ while particles scattered into a polar angle of $\arctan(\hat{\theta}_y/\hat{\theta}_x)$ and $\pi/2$ will be absorbed by the vertical aperture whenever the scattering angle exceeds this limit. We calculate the losses in only one quadrant of the polar variable and multiply the result by 4 since the scattering and absorption process is symmetric about the polar axis. The integral (11.107) becomes in this case

$$\begin{aligned}\int_{\hat{\theta}}^{\pi} \frac{\sin\theta\,\mathrm{d}\theta\,\mathrm{d}\varphi}{\sin^4(\theta/2)} = \quad & 4\int_0^{\arctan\left(\hat{\theta}_y/\hat{\theta}_x\right)} \mathrm{d}\varphi \int_{\hat{\theta}_x/\cos\varphi}^{\pi} \frac{\sin\theta\,\mathrm{d}\theta}{\sin^4(\theta/2)} \\ & + 4\int_{\arctan\left(\hat{\theta}_y/\hat{\theta}_x\right)}^{\pi/2} \mathrm{d}\varphi \int_{\hat{\theta}_y/\sin\varphi}^{\pi} \frac{\sin\theta\,\mathrm{d}\theta}{\sin^4(\theta/2)}\,.\end{aligned} \tag{11.114}$$

The solutions of the integrals are similar to that in (11.107) and we get

$$\int_{\hat{\theta}}^{\pi} \frac{\sin\theta \, \mathrm{d}\theta \, \mathrm{d}\varphi}{\sin^4(\theta/2)} = \frac{8}{\hat{\theta}_y^2} \left[\pi + \left(R^2+1\right) \sin(2 \arctan R) \right. \tag{11.115}$$

$$\left. +2\,(R-1) \arctan R\right] ,$$

where $R = \hat{\theta}_y/\hat{\theta}_x$.

Using (11.115) instead of (11.107) in (11.109) gives a more accurate expression for the beam lifetime due to Coulomb scattering. We note that for $R = 1$ we do not get exactly the lifetime (11.109) but find a lifetime that is larger by a factor of $1 + \pi/2$. This is because we used a rectangular aperture in (11.115) compared to a circular aperture in (11.107). The beam lifetime (11.112) becomes now for a rectangular acceptance

$$\tau_{\mathrm{cs}}(\mathrm{hours}) = 10.25 \, \frac{2\pi}{F(R)} \, \frac{(cp)^2(\mathrm{GeV}^2)\, \epsilon_{\mathrm{A}}(\mathrm{mm\,mrad})}{\langle\beta(\mathrm{m})\rangle \, P(\mathrm{nTorr})} \, . \tag{11.116}$$

The function $F(R)$

$$F(R) = [\pi + (R^2+1)\sin(2\arctan R) + 2(R^2-1)\arctan R \tag{11.117}$$

is shown in Fig. 11.5. For some special cases the factor $2\,\pi/F(R)$ assumes the values

shape of aperture	round	square	rectangular
ratio: $R = \hat{\theta}_y/\hat{\theta}_x$	1.00	1.00	$0 \rightarrow 1$
$2\pi/F(R)$	1.00	1.22	$2 \rightarrow 1.22$

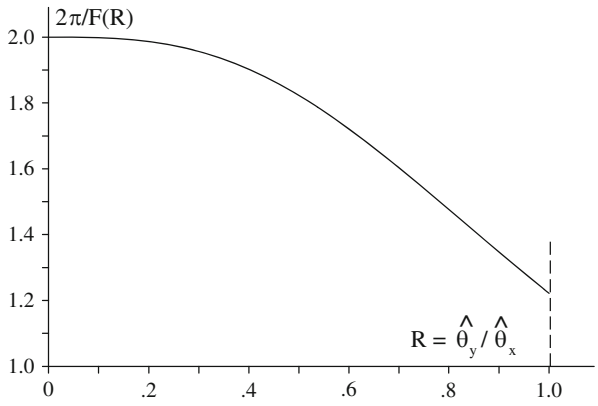

Fig. 11.5 Function $F(R)$ to determine the acceptance for Coulomb scattering

Tacitly we have assumed that the vertical acceptance is smaller than the horizontal acceptance which in most cases is true. In cases, where $\hat{\theta}_y > \hat{\theta}_x$, we may use the same equations with x and y exchanged.

Particles performing large amplitude betatron oscillations form a Coulomb scattering halo around the beam proper. In case of an electron storage ring the particle intensity in this halo reaches an equilibrium between the constant supply of scattered electrons and synchrotron radiation damping.

The deviation of the particle density distribution from a Gaussian distribution due to scattering can be observed and measured. In Fig. 11.6 beam lifetime measurements are shown for an electron beam in a storage ring as a function of a variable ring acceptance as established by a movable scraper. The abscissa is the actual position of the scraper during the beam lifetime measurement, while the variable for the ordinate is the aperture for which a pure Gaussian particle distribution would give the same beam lifetime.

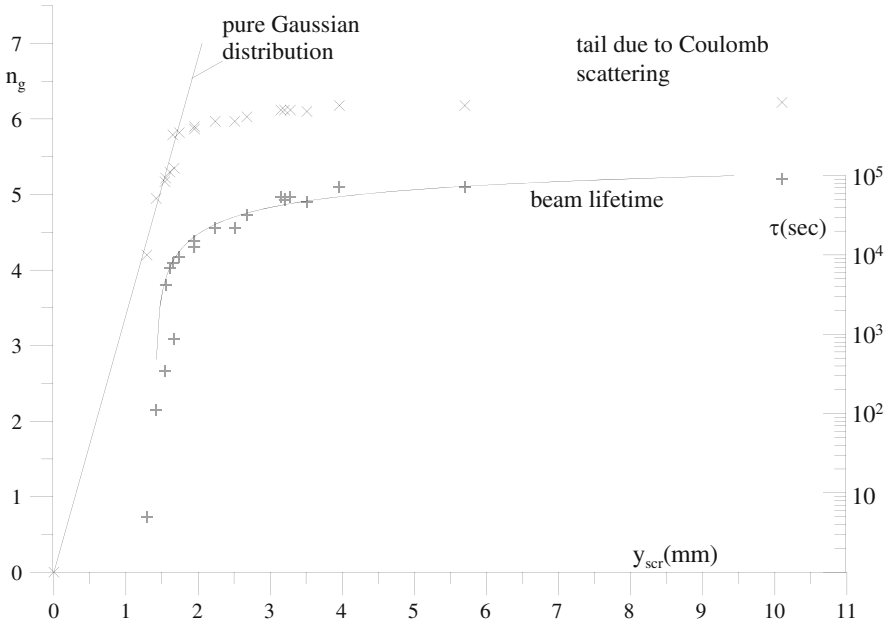

Fig. 11.6 Measurement of beam lifetime in an electron storage ring with a movable scraper. The *curve on the left* shows the Coulomp scattering halo for amplitudes larger than 6σ indicating a strong deviation from Gaussian particle distribution. the *curve on the right* shows the beam life time as a function of scraper position

If the particle distribution had been purely Gaussian the measured points would lie along a straight line. In reality, however, we observe an overpopulation of particles in the tails of the distribution for amplitudes larger than about 6σ forcing the scraper to be located farther away from the beam center to get a beam lifetime equal to that of a pure Gaussian distribution. This overpopulation or halo at large amplitudes is due to elastic Coulomb scattering on the residual gas atoms.

Since the acceptance of the storage ring is proportional to the square of the aperture at the scraper, we expect the beam lifetime due to Coulomb scattering to vary proportional to the square of the scraper position. This is shown in Fig. 11.7 for good vacuum and poor vacuum conditions. In the case of poor vacuum we find a saturation of the beam lifetime at large scraper openings which indicates that the scraper is no longer the limiting aperture in the ring. This measurement therefore allows an accurate determination of the physical ring acceptance or the dynamic aperture whichever is smaller.

So far we have assumed the residual gas to consist of homogeneous two atom molecules. This is not an accurate description of the real composition of the residual gas although on average the residual gas composition is equivalent to a nitrogen gas. Where the effects of a more complex gas composition becomes important, we apply (11.109) to each different molecule and atom of the residual gas and we replace the relevant factor PZ^2 by a summation over all gas components. If P_i is

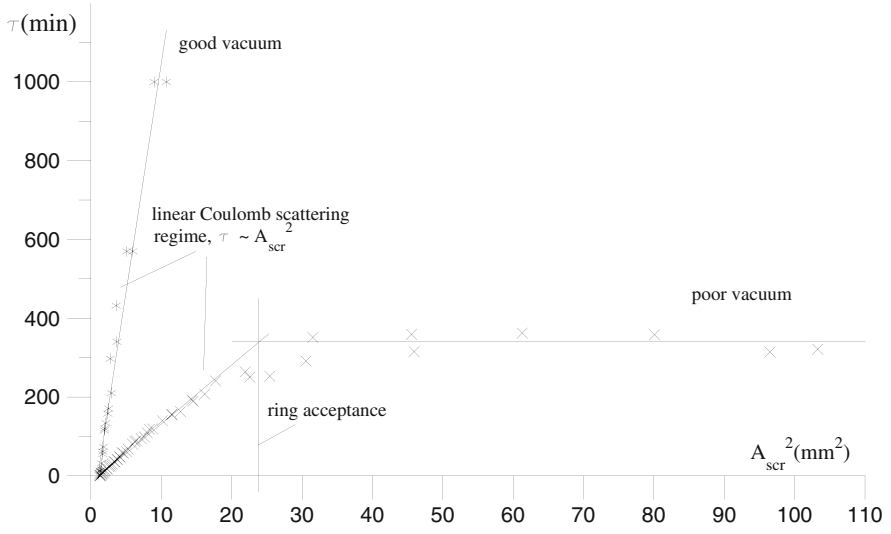

Fig. 11.7 Beam lifetime in an electron storage ring as a function of the acceptance. The transition of the *curve on the right* from a linear dependence of beam lifetime on the acceptance to a constant life time occurs when the acceptance due to the scraper position is equal to the ring acceptance

the partial pressure of the molecules i and Z_j the atomic number of the atom j in the molecule i we replace in (11.109)

$$PZ^2 \rightarrow \sum_{i,j} P_i Z_j^2 \tag{11.118}$$

and sum over all atoms i in the molecule j.

Inelastic Scattering

Charged particles passing through matter become deflected by strong electrical fields from the atomic nuclei. This deflection constitutes an acceleration and the charged particles lose energy through emission of radiation which is called bremsstrahlung. If this energy loss is too large such that the particle energy error becomes larger than the storage ring energy acceptance the particle gets lost. We are therefore interested to calculate the probability for such large energy losses to estimate the beam lifetime.

The probability to suffer a relative energy loss $\delta = \mathrm{d}E/E_0$ due to such an inelastic scattering process has been derived by Bethe and Heitler [16, 17]. For extreme relativistic particles and full screening this probability per unit thickness of matter is [17]

$$\mathrm{d}P = 2\overline{\Phi} n \frac{\mathrm{d}\delta}{\delta} (1-\delta) \left[\left(\frac{2 - 2\delta + \delta^2}{1-\delta} - \frac{2}{3} \right) 2 \ln \frac{183}{Z^{1/3}} + \frac{2}{9} \right], \tag{11.119}$$

where n is the number of atoms per unit volume and the factor $\overline{\phi}$ is with the fine structure constant $\alpha = 1/137$

$$\overline{\Phi} = r_\mathrm{e}^2 Z^2 \alpha \,. \tag{11.120}$$

We integrate this probability over all energy losses larger than the energy acceptance of the storage ring $\delta \geq \delta_\mathrm{acc}$ and get after some manipulation and setting $\delta_\mathrm{acc} \ll 1$

$$\begin{aligned} P &= 2\overline{\Phi}\, n \int_{\delta_\mathrm{acc}}^{1} \frac{\mathrm{d}\delta}{\delta} (1-\delta) \left[\left(\frac{2 - 2\delta + \delta^2}{1-\delta} - \frac{2}{3} \right) 2 \ln \frac{183}{Z^{1/3}} + \frac{2}{9} \right] \\ &\approx \frac{3}{4} (-\ln \delta_\mathrm{acc}) \left(4 \ln \frac{183}{Z^{1/3}} + \frac{3}{9} \right) n\overline{\Phi} \,. \end{aligned} \tag{11.121}$$

The radiation length L_r is defined as the distance over which the particle energy has dropped to $1/e$ due to inelastic scattering. For highly relativistic particles this length is given by [17]

$$\frac{1}{L_r} = \overline{\Phi}\, n \left(4 \ln \frac{183}{Z^{1/3}} + \frac{2}{9} \right) . \tag{11.122}$$

Combining (11.121) and (11.122), we find the simple solution that the probability for a particle to suffer a relative energy loss of more than δ_{acc} per radiation length is

$$P_{rad} = -\frac{4}{3} \ln \delta_{acc} . \tag{11.123}$$

To calculate the beam lifetime or beam decay rate due to bremsstrahlung we note that the probability for a particle loss per unit time is equal to the beam decay rate or equal to the inverse of the beam lifetime. The bremsstrahlung lifetime is therefore

$$\tau_{bs}^{-1} = -\frac{1}{N_0} \frac{dN}{dt} = P \frac{c}{L_r} = -\frac{4}{3} \frac{c}{L_r} \ln \delta_{acc} . \tag{11.124}$$

The radiation length for gases are usually expressed for a standard temperature of 20 °C and a pressure of 760 Torr. Under vacuum conditions the radiation length of the residual gas is therefore increased by the factor $760/P_{Torr}$. We recognize again the complex composition of the residual gas and define an effective radiation length by

$$\frac{1}{L_{r,eff}} = \sum_i \frac{1}{L_{r,i}} , \tag{11.125}$$

where $L_{r,i}$ is the radiation length for gas molecules of type i. The beam lifetime due to bremsstrahlung for a composite residual gas is from (11.124), (11.125)

$$\tau_{bs}^{-1} = -\frac{4}{3} c \sum_i \frac{1}{760} \frac{\tilde{P}_i}{L_{r,i}} \ln \delta_{acc} , \tag{11.126}$$

where $\tilde{P}_i$ is the residual partial gas pressure for gas molecules of type i. Although the residual gas of ultra high vacuum systems rarely includes a significant amount of nitrogen gas, the average value for $\langle Z^2 \rangle$ of the residual gas components is approximately 50 or equivalent to nitrogen gas. For all practical purposes we may therefore assume the residual gas to be nitrogen with a radiation length under normal conditions of $L_{r,N_2} = 290\,\text{m}$ and scaling to the actual vacuum pressure P_{vac} we get for the beam lifetime

$$\tau_{bs}^{-1}(\text{hours}^{-1}) = 0.00653\, P_{vac}(\text{nTorr}) \ln \frac{1}{\delta_{acc}} . \tag{11.127}$$

Basically the bremsstrahlung lifetime depends only on the vacuum pressure and the energy acceptance and the product of beam lifetime and vacuum pressure is a function of the energy acceptance $\delta_{\text{acc}} = \Delta\gamma/\gamma$,

$$\tau_{\text{bs}}(\text{hour})\, P(\text{nTorr}) = \frac{153.14}{\ln(\gamma/\Delta\gamma)}\,. \tag{11.128}$$

In tabular form we get:

$\delta_{\text{acc}} = \Delta\gamma/\gamma$	0.005	0.010	0.015	0.020	0.025
$\tau(\text{hr})\, P(\text{nTorr})$	28.90	33.25	36.46	39.15	41.51

There are many more forms of interaction possible between energetic particles and residual gas atoms. Chemical, atomic, and nuclear reactions leading to the formation of new molecules like ozone, ionization of atoms or radioactive products contribute further to energy loss of the beam particles and eventual loss from the beam. These effects, however, are very small compared to Coulomb scattering or bremsstrahlung losses and may therefore be neglected in the estimation of beam lifetime.

11.8.2 Ultra High Vacuum System

Accelerated particles interact strongly with residual gas atoms and molecules by elastic and inelastic collisions. To minimize particle loss due to such collisions we provide an evacuated beam pipe along the desired beam path. For open beam transport systems high vacuum of 10^{-5}–10^{-7} Torr is sufficient. This is even sufficient for pulsed circular accelerators like synchrotrons, where the particles remain only for a short time. In storage rings, however, particles are expected to circulate for hours and therefore ultra high vacuum conditions must be created.

Thermal Gas Desorption

To reach very low gas pressures in the region of 10^{-10}–10^{-11} Torr in the regime of ultra high vacuum (UHV) we must consider the continuous desorption of gas molecules from the walls due to thermal desorption. Gas molecules adsorbed on the chamber surface are in thermal equilibrium with the environment and the thermal energy of the molecules assumes a statistically determined Boltzmann distribution. This distribution includes a finite probability for molecules to gain a large enough amount of energy to overcome the adsorption energy and be released from the wall.

The total gas flow from the wall due to this thermal gas desorption depends mostly on the preparation of the material. While for carefully cleaned surfaces the thermal desorption coefficient may be of the order of 10^{-12}–10^{-13} Torr lt/sec/cm^2 a bakeout to 140–300 °C can reduce this coefficient by another order of magnitude.

Synchrotron Radiation Induced Desorption

In high-energy electron or positron accelerators a significant amount of energy is emitted in form of synchrotron radiation. This radiation is absorbed by vacuum chamber walls and causes not only a heating effect of the chamber walls but also the desorption of gas molecules adsorbed on the surface.

The physical process of photon induced gas desorption evolves in two steps [18]. First a photon hitting the chamber walls causes a secondary electron emission with the probability $\eta_e(\varepsilon)$, where ε is the photon energy. Secondly, the emission as well as the subsequent absorption of that photoelectron can desorb neutral atoms from the chamber surface with the probability η_d. To calculate the total desorption in a storage ring, we start from the differential synchrotron radiation photon flux (24.56) which we integrate over the ring circumference and write now in the form

$$\frac{\mathrm{d}N(\varepsilon)}{\mathrm{d}t} = \frac{8\pi\alpha}{9}\gamma\frac{I_\mathrm{b}}{e}\frac{\Delta\omega}{\omega}S(\zeta)\,, \tag{11.129}$$

where $\varepsilon = \hbar\omega$ is the photon energy, I_b the beam current, E the beam energy and $S(\zeta)$ a mathematical function defined by (24.57).

The photoelectron current $\dot{N}_\mathrm{e}$ results from the folding of (11.129) with the photoelectron emission coefficient $\eta_e(\omega)$ for the material used to construct the vacuum chamber and the integration over all photon energies,

$$\dot{N}_\mathrm{e} = \frac{8\pi\alpha}{9\,e\,mc^2}EI_\mathrm{b}\int_0^\infty \frac{\eta_\mathrm{e}(\omega)}{\omega}S\left(\frac{\omega}{\omega_c}\right)\mathrm{d}\omega\,. \tag{11.130}$$

The photoelectron emission coefficient depends on the choice of the material for the vacuum chamber. Figure 11.8 displays the photoelectron coefficient for aluminum as a function of photon energy [19].

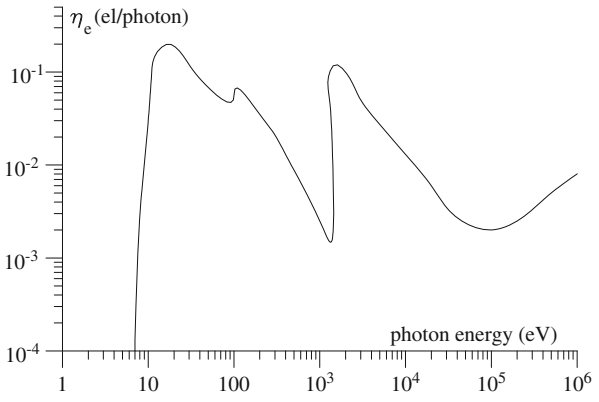

Fig. 11.8 Photon electron coefficient η_e for aluminum [19]

We note there are virtually no photoelectrons for photon energies of less than 10 eV. At 1,460 eV the K-edge of aluminum causes a sharp increase of the coefficient followed by a monotonous decrease for higher photon energies.

The photoelectron coefficient depends not only on the material of the photon absorber but also on the incident angle. The probability to release an electron from the surface is increased for shallow incidence of the photon. The enhancement factor $F(\Theta)$ represents the increase in the photoelectron-emission coefficient $\eta_e(\epsilon)$ due to a non normal incidence of a photon on the surface, where Θ is the angle between the photon trajectory and the plane to the absorbing surface. For angles close to normal incidence ($\Theta = 90°$) the enhancement factor scales like the inverse of the sine of the angle

$$F(\Theta) = \frac{1}{\sin\Theta}\,. \tag{11.131}$$

For small angles, however, the enhancement factor falls off from the inverse sine dependence as has been determined by measurements [20] and reaches a maximum value of about seven for small angles. The gas production is determined by the desorption rate Q, defined as the total number of neutral atoms released along the circumference from the chamber surface,

$$Q = 2\,\frac{22.4 \times 760}{6 \times 10^{23}}\,\dot{N}_e\;\eta_d\,, \tag{11.132}$$

where Q is expressed in Torr lt/sec and η_d is the desorption coefficient. The factor 2 is due to the fact that a photo electron can desorb an atom while leaving or arriving at a surface. With (11.132) we get the average vacuum pressure $\langle P\rangle$ from

$$\langle P\rangle = \frac{Q}{S}\,, \tag{11.133}$$

where S is the total installed pumping speed in the storage ring. For a reasonably accurate estimate of the photon flux we may use the small argument approximation (24.60) for photon energies $\varepsilon \le \varepsilon_c$. Photons of higher energies generally do not contribute significantly to the desorption since there are only few. To obtain the photon flux we therefore need to integrate only from 10 eV to $\epsilon \approx \epsilon_c$ the differential photon flux (24.60) folded with the photoelectron-emission coefficient $\eta_e(\varepsilon)$.

The desorption coefficient η_d is largely determined by the treatment of the vacuum chamber like baking, beam cleaning, argon discharge cleaning, etc. For example in the aluminum chamber of the storage ring SPEAR [21] the desorption coefficient at 1.5 GeV was initially about $\eta_d \approx 5 \times 10^{-3}$ then 5×10^{-4} after 1 month of operation, 10^{-4} after 2 months of operation and reached about 3×10^{-6} after about 1 year of operation. These numbers are not to be viewed too generally, since the cleaning process depends strongly on the particular preparation of the surfaces. However, following well established cleaning procedures and handling of ultra high vacuum components these numbers can be of general guidance consistent with observations on other storage rings.

Laboratory measurements [19] show the following relationship between photoelectron current $I_{\mathrm{phe}} = e\,\dot{N}_{\mathrm{e}}$, desorption coefficient η_{d} and total integrated beam time of a vacuum system

$$\eta_{\mathrm{d}} = 7 \times 10^{-5}\,\frac{I_{\mathrm{phe}}(\mathrm{A})}{t(\mathrm{hr})^{0.63}}\,. \tag{11.134}$$

New vacuum chambers release much gas when the first synchrotron radiation strikes the surface, but cleans quickly as the radiation cleaning continues.

Problems

11.1 (S). The Rf-frequency of a storage ring is 500 MHz. Every bucket is filled with particles. What is the time difference between successive bunches?

11.2 (S). Calculate the synchrotron damping time for a 3 GeV storage ring with a bending radius of $\rho = 10\,\mathrm{m}$ and pure rectangular dipole magnets. Assume 100 % bending magnet fill factor. What is the synchrotron damping time in this ring? How long does it take to radiate away all its energy?

11.3. Consider a circular electron storage ring of your choice and specify beam energy, current, ring circumference and average vacuum chamber dimensions. Calculate the total thermal gas desorption and the total required pumping capacity in the ring. Now add synchrotron radiation and estimate the increase of pumping speed needed after say 100 Ah of beam operation. Plot the average gas pressure as a function of integrated beam time.

11.4. An electron beam circulating in a 1.5 GeV storage ring emits synchrotron radiation. The rms emission angle of photons is $1/\gamma$ about the forward direction of the particle trajectory. Determine the photon phase space distribution at the source point and at a distance of 10 m away while ignoring the finite particle beam emittance. Now assume a Gaussian particle distribution with a horizontal beam emittance of $\epsilon_x = 1.5 \times 10^{-7}$ rad m. Fold both the photon and particle distributions and determine the photon phase space distribution 10 m away from the source point if the electron beam size is $\sigma_x = 1.225\,\mathrm{mm}$, the electron beam divergence $\sigma_{x'} = 0.1225\,\mathrm{mrad}$ and the source point is a symmetry point of the storage ring. Assume the dispersion function to vanish at the source point. For what minimum photon wavelength would the vertical electron beam size appear diffraction limited if the emittance coupling is 10 %?

11.5. Consider an electron beam in an isomagnetic 6 GeV storage ring with a bending radius of $\rho = 20\,\mathrm{m}$. Calculate the rms energy spread σ_ε/E_0 and the synchrotron oscillation damping time τ_s.

References

1. B. Touschek, in *Proceedings of 1963 Summer Study on Storage Rings, Acceleration and Experiment at Super High Energies*, vol. BNL-Report 7534 (Brookhaven BNL, New York, 1956), p. 171
2. A. Piwinski, in *9th International Conference on High Energy Accelerators* (Stanford Linear Accelerator Center, Stanford, 1974), p. 405
3. J.D. Bjorken, S.K. Mtingwa, Part. Accel. **13**, 115 (1983)
4. K.W. Robinson, Phys. Rev. **111**, 373 (1958)
5. M. Sands, Phys. Rev. **97**, 470 (1955)
6. D. Deacon, Theory of the isochronous storage ring laser. Ph.D. thesis, Stanford University, Stanford, 1979
7. C. Pellegrini, D. Robin, Nucl. Instrum. Methods **A301**, 27 (1991)
8. H. Wiedemann, Technical Report, PEP-Note 48, Stanford Linear Accelerator Center, Stanford (1973)
9. J.M. Paterson, J.R. Rees, H. Wiedemann, Technical Report, PEP-Note 125, Stanford Linear Accelerator Center, Stanford (1975)
10. S. Tazzari, *Electron Storage Rings for the Production of Synchrotron Radiation* Lecture Notes of Physics, vol. 296 (Springer, Berlin/Heidelberg, 1986), p. 140
11. H. Wiedemann, *Low Emittance Storage Ring Design*. Lecture Notes of Physics, vol. 296 (Springer, Berlin/Heidelberg, 1986), p. 390
12. K. Robinson, G.A. Voss, in *Proceedings of the International Conference on Electron and Positron Storage Rings* (Presses Universitaires de France, Paris, 1966), p. III–4
13. W.K.H. Panofsky, W.A. Wenzel, Rev. Sci. Instrum. **27**, 967 (1956)
14. V.L. Highland, Nucl. Instrum. Methods **129**, 497 (1975)
15. V.L. Highland, Nucl. Instrum. Methods **161**, 171 (1979)
16. H. Bethe, Proc. Camb. Phil. Soc. **30**, 524 (1934)
17. W. Heitler, *The Quantum Theory of Radiation* (Clarendon, Oxford, 1954)
18. E. Garwin, in *Proceedings of the 4th International Vacuum Congress* (Institute of Physics and the Physical Society, London, 1968), p. 131
19. J. Kouptsidis, A.G. Mathewson, Technical Report, DESY 76/49, DESY, Hamburg (1976)
20. O. Gröbner, A.G. Mathewson, P. Strubin, Technical Report, LEP-VAC/AGM/sm, CERN, Geneva (1983)
21. D. Bostic, U. Cummings, N. Dean, B. Jeong, J. Jurow, IEEE Trans. Nucl. Sci. **22**, 1540 (1975)